



Naturalis Repository

## Seasonality and lake water temperature inferred from the geochemistry and sclerochronology of quaternary freshwater bivalves from the Turkana Basin, Ethiopia and Kenya

Andrew S. Cohen, Julia Manobianco, David L. Dettman, Bryan A. Black, Catherine Beck, Craig S. Feibel, Josephine C. Joordens, Bert Van Bocxlaer, Hubert Vonhof

**Downloaded from**

[Naturalis Repository](#)

### **Article 25fa Dutch Copyright Act (DCA) - End User Rights**

This publication is distributed under the terms of Article 25fa of the Dutch Copyright Act (Auteurswet) with consent from the author. Dutch law entitles the maker of a short scientific work funded either wholly or partially by Dutch public funds to make that work publicly available following a reasonable period after the work was first published, provided that reference is made to the source of the first publication of the work.

This publication is distributed under the Naturalis Biodiversity Center 'Taverne implementation' programme. In this programme, research output of Naturalis researchers and collection managers that complies with the legal requirements of Article 25fa of the Dutch Copyright Act is distributed online and free of barriers in the Naturalis institutional repository. Research output is distributed six months after its first online publication in the original published version and with proper attribution to the source of the original publication.

You are permitted to download and use the publication for personal purposes. All rights remain with the author(s) and copyrights owner(s) of this work. Any use of the publication other than authorized under this license or copyright law is prohibited.

If you believe that digital publication of certain material infringes any of your rights or (privacy) interests, please let the department of Collection Information know, stating your reasons. In case of a legitimate complaint, Collection Information will make the material inaccessible. Please contact us through email: [collectie.informatie@naturalis.nl](mailto:collectie.informatie@naturalis.nl). We will contact you as soon as possible.



## Seasonality and lake water temperature inferred from the geochemistry and sclerochronology of quaternary freshwater bivalves from the Turkana Basin, Ethiopia and Kenya

Andrew S. Cohen<sup>a,\*</sup>, Julia Manobianco<sup>b</sup>, David L. Dettman<sup>a,c</sup>, Bryan A. Black<sup>d</sup>, Catherine Beck<sup>e</sup>, Craig S. Feibel<sup>f</sup>, Josephine C. Joordens<sup>g</sup>, Bert Van Bocxlaer<sup>h</sup>, Hubert Vonhof<sup>i</sup>

<sup>a</sup> Department of Geosciences, University of Arizona, Tucson, AZ, 85721, USA

<sup>b</sup> Department of Transportation, State of Arizona, Tucson, AZ, 85713, USA

<sup>c</sup> Estuary Research Center, Shimane University, Matsue, 690-8504, Japan

<sup>d</sup> Laboratory of Tree Ring Research, University of Arizona, Tucson, AZ, 85721, USA

<sup>e</sup> Geosciences Department, Hamilton College, Clinton, NY, 13323, USA

<sup>f</sup> Department of Earth and Planetary Sciences, Rutgers University, Busch Campus, Piscataway, NJ, 08854, USA

<sup>g</sup> Naturalis Biodiversity Center, 2333 CR, Leiden, the Netherlands

<sup>h</sup> CNRS, Univ. Lille, UMR 8198-Evo-Eco-Paleo, F-59000, Lille, France

<sup>i</sup> Max Planck Institute for Chemistry, 55128, Mainz, Germany

### ARTICLE INFO

Handling editor: Giovanni Zanchetta

#### Keywords:

Sclerochronology  
Stable isotopes  
Clumped isotopes  
Paleotemperature  
Lake turkana  
Turkana basin  
Climate variability  
Seasonality

### ABSTRACT

Reconstructing past environmental variability at short (annual-decadal) time scales is critical for understanding ecosystem change and ecological drivers of evolution. One promising approach to reconstructing that variability is through the use of stable isotope geochemistry and sclerochronology, the study of growth banding in organisms that undergo accretionary growth. We used a combination of sclerochronology, conventional stable isotope ratios and clumped isotope paleotemperatures to improve our understanding of past seasonality and climate variability in the Turkana Basin (Kenya, Ethiopia), which experiences a highly seasonal (tropical semi-desert) climate. In this case study, we apply these approaches to both Early Pleistocene and Holocene bivalve shells (*Etheria* and *Pseudobovaria*) to develop a model using various proxies of seasonal-interannual temporal variability in lake temperature and isotope chemistry. We leverage this model to better understand how lakes in the Turkana Basin have changed over short time-scales in the past. One modern (1979) river oyster has exclusively negative  $\delta^{18}\text{O}$  values through  $\sim 1.5$  yrs of growth and clumped isotope temperature reconstructions ( $30.1\text{--}31.5$  °C) consistent with a river delta provenance. Late Holocene shells show a wider range of isotopic variability within each shell's growth history than the modern sample ( $\sim 2\text{‰}$  for the modern sample vs.  $5\text{--}7\text{‰}$  for the Late Holocene samples) and near modern paleotemperatures, suggesting growth under both seasonal Omo flood pulse and lacustrine conditions. Middle Holocene shells exhibit less  $\delta^{18}\text{O}$  variability, consistent with growth in fresher Lake Turkana water at the end of the African Humid Period (12-5 ka), and with both surface water temperatures and water column temperature range similar to the Late Holocene. The Early Pleistocene shells have large seasonal  $\delta^{18}\text{O}$  cycles ( $4\text{--}7\text{‰}$ ), with  $\delta^{18}\text{O}$  values comparable to modern and Holocene deltaic shells, and a large range of paleotemperatures ( $21.8\text{--}31.3$  °C, including temperatures notably cooler than those measured in the modern lake:  $25\text{--}31$  °C), reflecting growth under significant seasonality in paleo-Omo River runoff. Oxygen isotope cycles suggest high degrees of seasonality of the paleo-Omo River runoff (or that of other major influents) into paleolake Lorenyang at  $\sim 1.6$  Ma, which may be similar to modern hydroclimate conditions. Comparison to prior datasets from nearby outcrops in the same basin suggests an increase in hydroclimate seasonality between 1.9 and 1.6 Ma. The combination of clumped isotope paleotemperature estimates from shallow water species such as *E. elliptica* with  $\text{TEX}_{86}$  measurements (derived here from previously published, contemporaneous sediment core studies from the south basin of Lake Turkana), which record temperatures near the oxycline, may provide a new approach to estimating past temperature variability along a vertical profile in

\* Corresponding author.

E-mail address: [cohen@email.arizona.edu](mailto:cohen@email.arizona.edu) (A.S. Cohen).

<https://doi.org/10.1016/j.quascirev.2023.108284>

Received 10 December 2022; Received in revised form 5 August 2023; Accepted 21 August 2023

Available online 31 August 2023

0277-3791/© 2023 Elsevier Ltd. All rights reserved.

lakes, thereby providing information on water column mixing regimes. Our approach greatly expands our toolkit for understanding coupled climate seasonality and variability in the Turkana Basin.

## 1. Introduction

The role that environmental variability, especially of climate, may have played in generating thermal and moisture stresses, and thereby structuring ecosystem and evolutionary change, is debated across a wide range of disciplines (Potts, 1996; Grove, 2011; Potts and Faith, 2015; Maxwell et al., 2018; Joordens et al., 2019; Faith et al., 2021; Cohen et al., 2022). Quantitative reconstructions of past environmental variability can come from a wide variety of paleorecords (e.g. pollen, paleosol isotopes, diatoms), can be constructed from various types of archives (e.g., outcrop records, and marine or continental drill core records), and may be assessed over a wide range of temporal scales. Our toolkit for obtaining records of seasonal to decadal changes in temperature and water chemistry in aquatic environments, and especially in lakes, is rapidly expanding, which addresses the critical need for assessing how these ecosystems have responded in the past to both changes in seasonality and sub-decadal modes of climate variability and what changes in variation may imply for future change in aquatic ecosystems over similar time-scales (e.g., Escobar et al., 2010; Glaubke et al., 2021; Thirumalai et al., 2023).

One of the most critical components of variability from an organismal perspective is seasonality, a characteristic of a time series referring to periodic and generally regular and predictable changes that occur over a year. Seasonality (and its change over geological time) is widely recognized as a potential driver of ecosystem reorganization and evolution, including that of hominins (e.g. Kingston et al., 2007). In eastern Africa, the role of environmental variability in structuring the ecosystem context of human evolution has been particularly vigorously debated (Potts, 1996; Potts and Faith, 2015; Kingston et al., 2007; Grove, 2011; Potts and Faith, 2015; Cohen et al., 2022), and an important component of that debate pertains to the variability in various physico-chemical conditions that organisms experience over short time scales, i.e. from seasons to their lifespans. All organisms have physiological limitations in the extent to which they can tolerate seasonal variability in moisture and temperature, and extreme values may induce stress that can act as a selective agent in evolution. However, seasonality is not the only mode of short-term variability. For example, processes such as the *El Niño-Southern Oscillation* (ENSO) can amplify or otherwise alter seasonal intensity of precipitation and temperature over ~3–7 year cycles, and these lower frequency cycles also alter ecosystem functioning (Plisnier et al., 2000; Kaboth-Bahr et al., 2021).

Across the spectrum of high frequency change in climate (seasonal to sub-decadal), variability is difficult to reconstruct with most commonly used paleoenvironmental indicators. Consequently, our understanding of seasonality, especially in the Quaternary history of eastern Africa, remains very limited. Lake deposits and the fossils they contain are excellent archives for reconstructing the “hydroclimate” (reconstructing various aspects of the hydrological cycle, especially limnologic variables influenced by external climate drivers), and thus indirectly, for climate of Africa during the Quaternary (Cohen et al., 2016a). Techniques that can leverage the continuity of lake deposit records with indicators of hydroclimate seasonality are thus critical for understanding short-term environmental variability across a range of time scales.

Here we aim to gain insight into long-term changes in seasonality through the use of sclerochronology, the study of physical and chemical variations in incremental growth bands of freshwater bivalve shells, to reconstruct seasonal variability in eastern Africa during the Holocene and Pleistocene. It is well established that the stable oxygen isotope ratios of mollusk shells ( $\delta^{18}\text{O}_s$ ), if not diagenetically altered, mainly reflect the temperature and oxygen isotope ratio of the water ( $\delta^{18}\text{O}_w$ ) in which they grew (Epstein et al., 1953; Grossman and Ku, 1986; Dettman

et al., 1999). Therefore, freshwater bivalve  $\delta^{18}\text{O}_s$  data provide excellent opportunities for detecting seasonal hydroclimate changes as they allow us to reconstruct past water  $\delta^{18}\text{O}_w$  values and/or river discharge conditions over the bivalve’s life span, which typically covers several years (Kelemen et al., 2019). Our objective with this study is to investigate changes in seasonal hydroclimate in the Turkana Basin using bivalve sclerochronology to better understand the paleoenvironmental variability at various time intervals from the Early Pleistocene to the recent past. We have specifically chosen to conduct this project in the Turkana Basin because it is a region that has contributed prominently to our understanding of Quaternary ecosystem evolution in Africa, and how environmental change has in turn influenced hominin evolution (Wood and Leakey, 2011).

We also complement the well-established paleohydrological utility of sclerochronology with newly-developed methods of measuring clumped isotope paleothermometry (Yanay et al., 2022) on the same shells, enabling us to reliably reconstruct temperature and oxygen isotope signatures of past water conditions. This “proof-of-concept” combination of methods leverages the relatively small size of samples and rapid sample analysis allowed by tunable infrared laser differential absorption spectroscopy (TILDAS). TILDAS typically measures 1.9 mg  $\text{CaCO}_3$  at high precision (comparable to latest generation isotope ratio mass spectrometry), to make clumped isotope measurements, which is critical for the small sample masses available from incrementally-sampled shells. Using this new approach, future sclerochronology studies in all contexts will be able to analyze temperature variability more rapidly than has previously been possible. We recognize from the outset that, due to the proof-of-concept nature of our current study, the initial data set reported here is relatively small and lacks contemporaneous samples from all environments (lake, delta and Omo River) for each studied period. In the future, enhancing our sampling will allow a more comprehensive understanding of the paleohydrologic and thermal history for Lake Turkana and the previous paleolakes occupying the Turkana Basin. Furthermore, enhanced sampling would enable to reconstruct variation over decades or more, (e.g. from organisms that have longer life spans), so the methodologies for which we develop this proof-of-concept could be applied to investigate how water chemistry and water temperature in lakes can vary over longer time-scales, encompassing variability driven by factors such as the ENSO cycle.

Mollusk shell sclerochronology is a particularly useful approach to studying past seasonality in growth rates and ambient water chemistry or other limnological/oceanographic variables, as the wide geographic range of mollusks allows for a high-resolution reconstruction of environmental conditions across a wide range of environments, from marine to freshwater and across most climatic zones (Gröcke and Gillikin, 2008). Furthermore, the analysis of fossil shells allows for seasonal environmental reconstructions over a vast span of geologic time (Dettman et al., 2001; Fan and Dettman, 2009; Wang et al., 2020). In temperate climates, highly seasonal temperature variations often complicate the interpretation of growth banding and oxygen stable isotope sclerochronological results, as bivalves may cease growth during cold winter temperatures, or even resorb shell material during hibernation (e.g. Downing and Downing, 1993; Anthony et al., 2001). Additionally,  $\delta^{18}\text{O}_s$  values are a function of both water temperature and  $\delta^{18}\text{O}_w$  (Dettman et al., 1999; Hallman et al., 2013), which makes it difficult to distinguish isotopic variability as strictly a function of changing temperatures or hydrologic conditions. In permanent waterbodies in the tropics, minimal seasonality in temperature favors bivalve growth year-round, although some species in temporary waterbodies also estivate during dry seasons. Under such conditions,  $\delta^{18}\text{O}_s$



variability is primarily driven by seasonal variations in  $\delta^{18}\text{O}_\text{w}$  and lake water temperature. For example, the  $\delta^{18}\text{O}_\text{s}$  of fossil gastropods and bivalve shells have been used to reconstruct large changes in rainfall seasonality and enhanced monsoonal precipitation during the early

Holocene in northwest Sudan (Abell and Hoelzmann, 2000; Rodrigues et al., 2000). Although bivalve growth cessation can occur in the tropics for reasons of elevated temperatures, desiccation or unfavorable water chemistry and anoxia (e.g. Vonhof et al., 2013), such growth-stopping

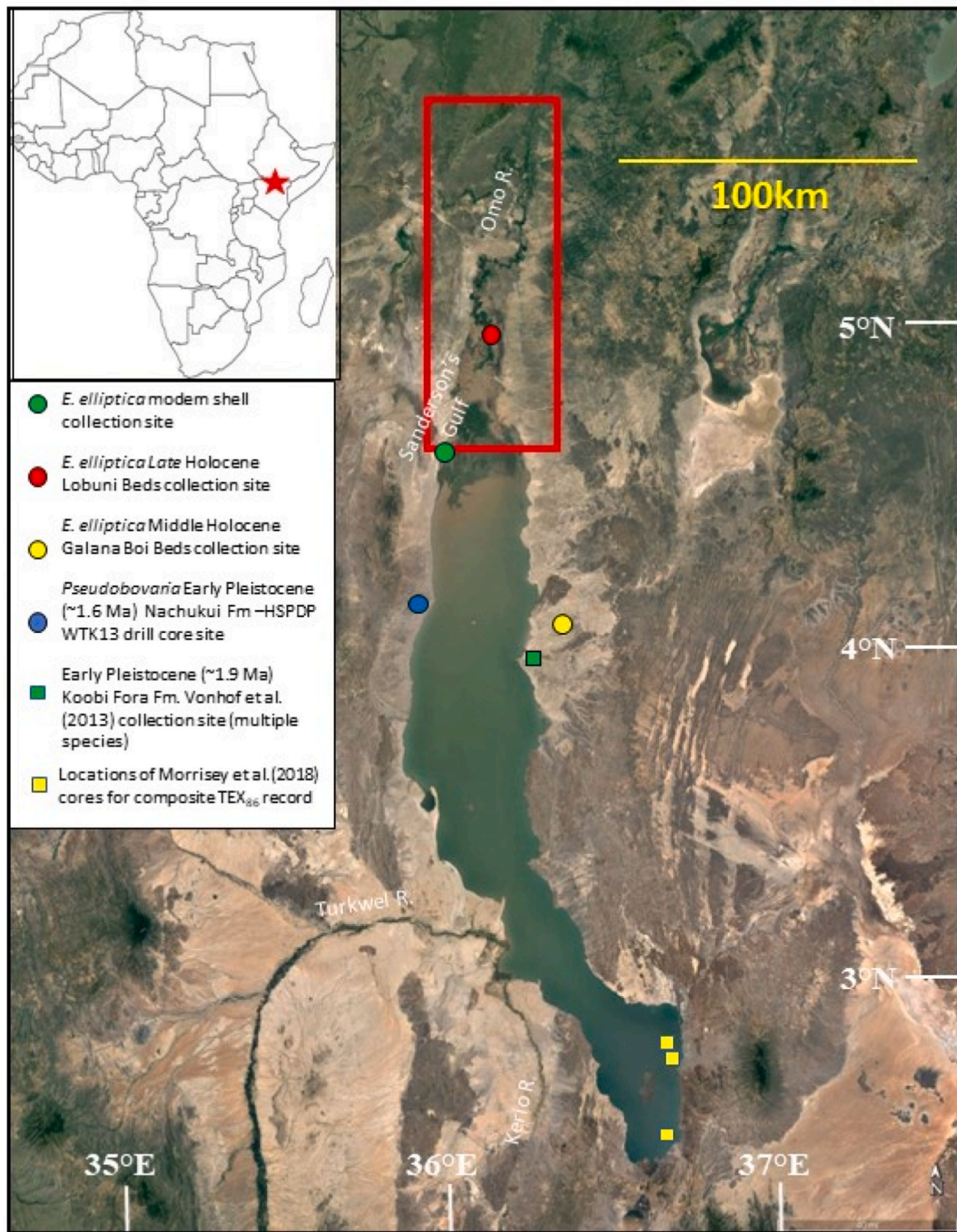


**Fig. 1.** Lake Turkana and the lower Omo River valley (red rectangle), showing location of the lake in Africa indicated on inset map by a red star. Modern *Etheria elliptica* collection location shown by a green circle. Approximate Late Holocene *E. elliptica* collection location in the Lower Omo River Valley (red circle, note exact lat./long. coordinates uncertain). Middle Holocene *E. elliptica* collection location (Galana Boi Beds) shown by a yellow circle and the HSPDP WTK13 drill core site, from which Early Pleistocene *Pseudobovaria* sp. fossils were collected, is located at the blue circle. Location of comparative Early Pleistocene samples from Vonhof et al. (2013) shown by green square (Koobi Fora Fm. Areas 100 and 102).



conditions may be less widespread and/or less frequent than at high latitudes.

In this study, we have constructed sclerochronological records from two bivalve species from Holocene and Early Pleistocene sediments from the Turkana Basin in eastern Africa: *Etheria elliptica*, the African river “oyster”, and *Pseudobovaria* sp., a small extinct unionid bivalve. We have studied shells of these species as seasonal hydroclimate archives by analyzing growth banding and stable isotope composition deposited in aragonite shell layers. Expanding upon research by [Vanhof et al. \(2013\)](#), which provided the first detailed sclerochronological study of mollusk stable isotopes from the Turkana Basin, the new oxygen isotope and growth data presented here, combined with reconstructions of paleotemperature allow us to investigate changes in the amplitude of hydrologic seasonality in lacustrine and riverine environments during the Holocene and Pleistocene in the Turkana Basin. This study aims to: (i) investigate the relationship between sclerochronology,  $\delta^{18}\text{O}$  values and the influence of seasonality on both in a tropical lake, (ii) use the seasonal  $\delta^{18}\text{O}_s$  values of bivalve mollusk shells to determine changes in amplitude of seasonal river discharge associated with changes in upstream monsoonal precipitation, and how these factors have varied over various timescales relevant to ecosystem change and evolution in eastern Africa, and (iii) link sclerochronological data with independently obtained paleotemperature data, using a newly developed, laser-spectroscopy-based clumped isotope data set on the same samples.

### 1.1. Modern environmental setting and climatology

Lake Turkana, the world’s largest desert lake, is located in the eastern branch of the East African Rift System (EARS) straddling the border of Kenya and Ethiopia ([Fig. 1](#)). The Lake Turkana watershed basin occupies 146,000 km<sup>2</sup>, extending from the Kenyan Highlands south of the lake near the equator to the Ethiopian Highlands north of the lake ([Johnson and Malala, 2009](#)). Lake Turkana is 250 km long and 30 km wide with mean and maximum depths of 35 m and 120 m, respectively ([Johnson and Malala, 2009](#)). The modern lake surface elevation is 362 m.a.s.l. ([Bloszies et al., 2015](#)). Lake Turkana is currently hydrologically closed, and is slightly saline (total dissolved solids = 2500 ppm) and moderately alkaline ([Yuretich and Cerling, 1983](#)).

Lake Turkana is located in the arid Turkana Depression with a mean annual air temperature of ~30 °C and a mean monthly temperature range of ~28–~32 °C ([Johnson and Malala, 2009](#); [Boës et al., 2018](#); [Morrissey et al., 2018](#)). Open-water lake surface temperatures (LST) range from 25 to 31 °C, with the warmest temperatures occurring in the north basin, and a maximum temperature gradient of 5 °C exists between surface and bottom waters ([Ferguson and Harbott, 1972](#); [Källqvist et al., 1988](#)). Measurements from the 1979 summer field season indicate a wider range of LSTs in both sheltered embayments in the north basin and Omo delta exposed to diurnal temperature swings, and in shallow waters affected by the seasonal Omo River plume, from 23 to 31 °C ([Table S1](#)) than offshore temperatures (25–31 °C). LSTs are 1–3.5 °C lower in July–December, when the lake is more strongly mixed, than during March–May, when stronger stratification of lake waters occurs and the position of the tropical rain belt increases cloud cover ([Ferguson and Harbott, 1972](#); [Källqvist et al., 1988](#)). Mean annual precipitation (MAP) in the Turkana Depression is ~200 mm/y, much less than the annual evaporation rate of ~2300 mm/y ([Yuretich and Cerling, 1983](#); [Johnson and Malala, 2009](#)). Precipitation over the lake occurs during two rainy seasons: the ‘long rains’ from March to May and the ‘short rains’ from October to November ([Nicholson, 1996](#); [Yang et al., 2015](#)). The Ethiopian Highlands receive >1500 mm/yr MAP, primarily during boreal summer ([Boës et al., 2018](#)). The Omo River supplies ~84% of freshwater input to Lake Turkana by draining the humid Ethiopian Highlands ([Avery and Tebbs, 2018](#)). The maximum precipitation over the Ethiopian Highlands during late boreal summer is coeval with maximum Omo River discharge during August and September ([Ethiopia Electric Power Corporation EEPCO, 2009](#); [Bloszies et al., 2015](#); [Avery](#)

[and Tebbs, 2018](#)). The remaining ~16% of freshwater input to the lake is contributed by the Kerio and Turkwel Rivers to the southwest, which drain the Kenyan Highlands ([Joordens et al., 2011](#)). Hydrothermal inputs to the lake are negligible ([van der Lubbe et al., 2017](#)). Therefore, today the Turkana Basin is hydrologically connected to two different precipitation modes, bimodal (spring and autumn) in the Kenyan Highlands and unimodal (summer) in the Ethiopian Highlands ([Yang et al., 2015](#); [Yost et al., 2021](#)).

Seasonal variation in lake water isotope ratios and lake water temperature in Turkana do not appear to occur in lock step. Isotopic composition is primarily driven by variability in upstream Omo River discharge, which brings river waters with lower  $\delta^{18}\text{O}$  values to the lake, where they mix with the more evaporative lake waters ([Thirumalai et al., 2023](#)). This Omo River discharge currently reaches its maximum in August and September ([Ferguson and Harbott, 1972](#); [Källqvist et al., 1988](#)), with only a short lag time from the maximum rainfall at the source in the Ethiopian Highlands. Elevated discharge causes lake levels and primary productivity to rise (the latter especially in the north basin). Air temperatures are highest in December–March and coolest in July–August ([Ferguson and Harbott, 1972](#); [Källqvist et al., 1988](#)). Open water temperature maxima lag slightly behind air temperatures (April–May), whereas the coolest water temperatures largely coincide with air temperature trends. These patterns can however be locally overprinted around river deltas if influent water temperatures differ substantially to those of open lake water.

The regional climatology of eastern Africa is controlled by a complex interplay between coupled ocean-atmosphere processes associated with both the Indian and Atlantic Oceans and the convective tropical rain belt ([Tierney et al., 2011](#)). The arid conditions in the Turkana Depression are associated with the low-level Turkana Jet, which funnels descending air over Lake Turkana via orographic channeling ([Nicholson, 1996](#)). Precipitation in both the surrounding Ethiopian and Kenyan highlands is seasonally variable with the annual meridional migration of the tropical rain belt ([Nicholson, 1996, 2018](#); [Johnson and Malala, 2009](#)). Low-level atmospheric divergence underlies much of the region of maximum rainfall ([Yang et al., 2015](#); [Nicholson, 2018](#)). [Yang et al. \(2015\)](#) identified orographic lifting, the seasonal cycle of moist static energy in the lower atmosphere, and vertically integrated moisture from the Indian Ocean as important factors contributing to equatorial eastern African precipitation. Atlantic Ocean moisture does not significantly contribute to precipitation over the modern Turkana Basin as the Congo Air Boundary (CAB), the convergence zone of air masses derived from the Atlantic and Indian Oceans, presently lies west of Lake Turkana ([Tierney et al., 2011](#); [Bloszies et al., 2015](#)). However, higher lake levels in the EARS during the African Humid Period (AHP, ~12–5 ka; an interval of increased precipitation and high lake levels throughout much of northern and tropical Africa, *sensu de Menocal et al., 2000*) may be attributed to increased rainfall due to an eastward shift of the CAB ([Tierney et al., 2011](#); [Morrissey and Scholz, 2014](#); [Junginger and Trauth, 2013](#); [Junginger et al., 2014](#); [van der Lubbe et al., 2017](#)).

### 1.2. Geologic setting and paleolakes

The Turkana Basin forms a portion of the East African Rift System (EARS), consisting of a series of north-south half grabens that has developed since at least the Miocene ([Tiercelin and Lezzar, 2002](#); [Feibel, 2011](#); [Nutz et al., 2020](#)). The most recent phase of sedimentary accumulation in the basin is related to the formation of modern Lake Turkana ~200 ka ([Feibel, 2011](#)). Desert lakes are particularly sensitive to hydroclimate variations and often amplify hydroclimatic signals. In the EARS, rift basin geometry and high evaporation rates have caused rapid lake level transgressions-regressions throughout the Quaternary ([Garcin et al., 2012](#); [van der Lubbe et al., 2017](#)). Over these transgressive-regressive cycles, Turkana paleolakes alternated from exorheic/fresher water conditions during highstands to endorheic/saline-alkaline water conditions during lowstands ([Boës](#)

et al., 2018; Beck et al., 2019; Nutz et al., 2020). The latter, endorheic state exists in the basin today. The documentation of quasi-modern bivalve isotopic conditions makes up one focal area of the sampling in this study.

During the Late Pleistocene and Holocene, several rapid lake level fluctuations have been documented in lacustrine outcrops, sediment cores and seismic reflections in the Turkana Basin (Garcin et al., 2012; Forman et al., 2014; Morrissey and Scholz, 2014; Bloszies et al., 2015). During the early Holocene AHP, Lake Turkana reached a maximum highstand of up to 100 m above modern lake level, overflowed into the White Nile River system, and was also hydrologically connected to the neighboring, upstream Suguta and Chew Bahir basins (Garcin et al., 2012; Morrissey and Scholz, 2014; Junginger et al., 2014; Foerster et al., 2015; Bloszies et al., 2015; Fischer et al., 2020). The exact timing of Lake Turkana highstands during the AHP is debated because of dating uncertainties and differing conclusions based on the source of individual lake level reconstructions (Bloszies et al., 2015; Beck et al., 2019). Samples from the latter part of the AHP make up a second component of the current study.

Paleolake transgressive-regressive cycles in the Turkana Basin are also observed over longer timescales in the lacustrine sedimentary record throughout the Plio-Pleistocene (Feibel, 2011; Boës et al., 2018; Nutz et al., 2017, 2020). Outcrop facies and sequence analysis by Nutz et al. (2020) suggests that Turkana paleolakes experienced seven high-amplitude transgression-regression cycles between ~4.00 and ~0.75 Ma. However, high resolution studies from the Hominin Sites and Paleolakes Drilling Project (HSPDP) West Turkana (Kenya) WTK13 drill core sediments (Fig. 1) suggest numerous paleolake level fluctuations on centennial to millennial timescales throughout the Quaternary (Cohen et al., 2022). The HSPDP research effort was designed to obtain high resolution sediment core records from sites close to important fossil hominin and archaeological localities in Kenya and Ethiopia, with the goal of providing a detailed paleoenvironmental and paleoclimatic context to key intervals of human evolution (Cohen et al., 2016a, 2022). Samples from the paleolake Lorenyang phase, which occurred between ~2.1 and ~1.3 Ma (Feibel, 2011), obtained from the HSPDP-WTK13 drill core form a third focus of this study.

## 2. Materials and methods

### 2.1. Riverine and lacustrine bivalve samples

This study uses two species of bivalves for geochemical and sclerochronological analysis. *Etheria elliptica* is an African river oyster, of the order Unionida and family Etheriidae (Van Bocxlaer and Van Damme, 2009; Elderkin et al., 2016). It was chosen for study here because of its common occurrence in the Turkana Basin fossil record. Modern *E. elliptica* live cemented to hard substrates in shallow flowing water or agitated lake shoreline environments and are widely distributed throughout African freshwater ecosystems, including multiple drainages in southern Saharan Africa, the Nile River drainage, the African Rift Lakes, and northern Madagascar (Mandahl-Barth, 1988; Abell et al., 1995; Van Bocxlaer and Van Damme, 2009). *Etheria elliptica* do not typically exceed 15 cm asymptotic length and 8 years of age (Akélé et al., 2015). Abell et al. (1995) suggested that *E. elliptica* accretionary growth bands form with a lunar-month periodicity but offered no biological explanation for synodic rhythm bivalve growth in an equatorial freshwater setting lacking significant tides. To the extent possible given the available fossils, we chose shells that did not show any apparent growth cessation or resorption, to produce as continuous an isotopic and growth record as possible from each, although we acknowledge that such growth patterns can be difficult to detect in all cases. *Pseudobovaria* sp. is a small extinct African mussel of the order Unionida and family Unionidae, which lived in well-oxygenated freshwater lakes during the Plio-Pleistocene (Van Bocxlaer, 2020). It was the most common fossil bivalve found in the WTK drill core.

A total of four *E. elliptica* single valves were collected from the Lower Omo River basin (Fig. 1). One modern shell (sample Ee Cohen 79) was collected on the northwestern shoreline of Lake Turkana very close to the Omo River delta in 1979, prior to the construction of major dams on the Omo River, which have altered the hydrology and seasonal cycle of Omo discharge substantially (Avery and Tebbs, 2018). Shells that grew after 2000 (and especially since the start of infilling of the largest dams in the mid-2010s) grew in a seasonal hydrologic and isotopic regime that is increasingly detached from the annual Omo River flood cycle, which limited the number of modern shells available to reconstruct baseline conditions for this study.

Three Late Holocene *Etheria* shells (samples Lobuni Ee1, Lobuni Ee 2 and Lobuni Ee 3; Fig. 2a) were collected from the Lobuni Beds, Lower Omo Channel in 1970 by Claudia Carr (Sample LO6903). The Lobuni Beds are the most recent alluvial, deltaic and littoral deposits of the Lower Omo River basin and were originally estimated on geomorphic grounds to be Late Holocene in age (Butzer and Thurber, 1969). These *Etheria* shells may have undergone some indeterminate amount of fluvial transport prior to deposition. Two Middle Holocene *E. elliptica* shells (fossils E2 and E3) were collected from the Galana Boi Beds in the Bakate Gap/Koobi Fora area east of Lake Turkana (4.05°N, 36.29°E) in August 2019 (Fig. 1), about 10 km north of the paleo-discharge area of upstream Chew Bahir overflow into Lake Turkana and ~40 m above the modern lake level.

Pleistocene lacustrine fossil shells were extracted from the HSPDP-WTK13 sediment core (Fig. 1). In 2013, a single borehole, deviated 10° from vertical, was cored to a depth of ~216 m in West Turkana (4.109721° N, 35.871783° E). Full coring details and initial core descriptions are presented in Cohen et al. (2016a). Lupien et al. (2018) developed an age model of the WTK13 core using tephra correlation, direct <sup>40</sup>Ar/<sup>39</sup>Ar dating of a new tephra and paleomagnetic reversal stratigraphy (Sier et al., 2017). The WTK13 core was sampled for bivalve shells in coquina intervals in June 2019 at the National Lacustrine Core Facility (LacCore), University of Minnesota. Core drive 31Q-2 yielded the largest and best-preserved fossil bivalve shells from two coquina layers (Fig. 2c and d) with an estimated age range of 1.634 Ma to 1.638 Ma based on the Lupien et al. (2018) age model. From each of these two coquina layers three *Pseudobovaria* sp. bivalve shells were chosen for sclerochronological and geochemical analysis. Unfortunately, no *E. elliptica* shells were found in the drill core samples. Because *Pseudobovaria* is an extinct genus we can only make limited paleoecological interpretations about its life habit and the degree to which non-equilibrium isotopic fractionation processes may have differed between this genus and *Etheria* is thus unknown. Due to the small (~1 cm umbo to ventral margin length) and fragile condition of the shells, *Pseudobovaria* sp. were embedded in epoxy resin and cut in half along the maximum growth axis for sclerochronological sampling of seasonal stable isotopes (Fig. 2b).

### 2.2. Raman spectroscopy

To examine whether diagenesis and mineralogic alteration potentially affected our older, Early Pleistocene shells, we used Raman spectroscopy to determine shell mineralogy. This work was conducted at the Mineralogy and Crystallography Laboratory, University of Arizona. The Raman spectra of two early Pleistocene *Pseudobovaria* sp. were collected on randomly oriented crystals on a Thermo Almega microRaman system, using a solid-state laser with a frequency of 532 nm and a thermoelectric cooled CCD detector. The laser is partially polarized with 4 cm<sup>-1</sup> resolution and a spot size of 1 μm (Yang et al., 2022). Freshwater bivalves such as *Pseudobovaria* sp. and *Etheria elliptica* produce calcium carbonate shells composed of aragonite. If the shells contain more stable calcite, this would be indicative of diagenesis, which would indicate that the shell geochemistry could not be used for paleoenvironmental analysis as it no longer reflects the hydrological environment in which primary carbonate formation took place.

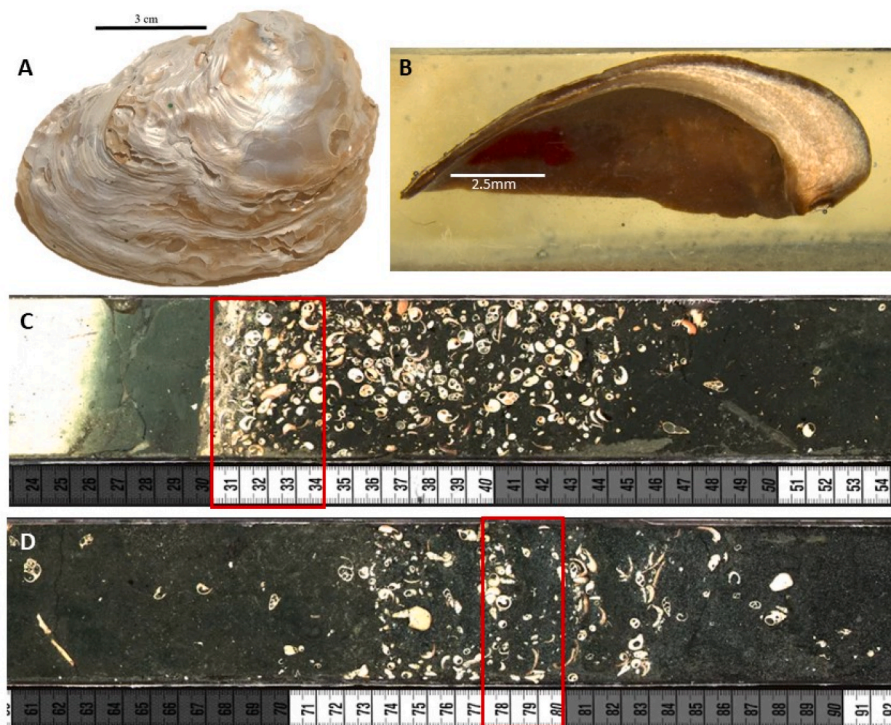


**Fig. 2.** Images of bivalves and core intervals sampled. A. Late Holocene *Etheria elliptica* Lobuni Ee 3. B. Cross section of Pleistocene *Pseudobovaria* sp. embedded in epoxy resin. C,D. The sampled shell lag intervals from HSPDP WTK13 1A-31Q-2. C: the shell lag interval at 31–34 cm; D: that at 78–80 cm (indicated in red boxes). Three shells were analyzed from each shell lag.

### 2.3. Radiocarbon age determination

For this study, all Holocene shells were radiocarbon-dated at the Accelerator Mass Spectrometry Laboratory, University of Arizona. All  $^{14}\text{C}$  ages were converted to calibrated ages in calendar years BP using OxCal with the IntCal20 calibration curve (Reimer et al., 2020). Because of the high exchange rate between  $\text{CO}_2$  in modern lake water and atmospheric  $\text{CO}_2$ ,  $^{14}\text{C}$  reservoir age correction is unnecessary for Middle Late Holocene Lake Turkana sediments (Halfman et al., 1994; Berke et al., 2012; Garcin et al., 2012; van der Lubbe et al., 2017).

### 2.4. Conventional stable isotope sampling and analysis

Prior to aragonite sampling, *E. elliptica* shells were submerged in an ultra-sonic cleaner for 15 min, whereas *Pseudobovaria* sp. shells were soaked in reverse osmosis water for 24 h to remove sediment debris. The shells were air dried at room temperature over 48–72 h. Because of the irregular shape and porous voids observed in fossil *E. elliptica* shells, small aragonite powder samples (~0.05 mg) were micro-drilled sequentially on the shells' exterior with a 0.3 mm drill bit for stable isotope analysis. For modern and Late Holocene specimens Ee Cohen 79 and Lobuni Ee 1–3, shell samples were drilled from the umbo to ventral margin in chronological order along visible growth laminae. The distance of drill holes along the maximum growth axis for specimens Ee Cohen 79 and Lobuni Ee 1–3 were measured using a flexible tape measure. Because of abrasion and difficulties in tracing growth along the outer surface it was necessary to take a slightly different sampling strategy for the Middle Holocene fossils E2 and E3: these shell samples were drilled chronologically along the hinge and drill hole distance was measured on microscopic images using the distance measuring tool in Leica Application Suite X. Between 15 and 34 stable isotope samples were taken from each *Etheria* shell.

Six *Pseudobovaria* sp. shell cross sections were micromilled in the prismatic and nacreous layers along growth laminae at a resolution of

~50–60  $\mu\text{m}$  using a GeoMill326 micromill. Between 26 and 48 isotope samples were collected on each *Pseudobovaria* shell. For micromilled *Pseudobovaria* sp., sequential drill hole numbers are reported rather than distances because of the continuous milling of samples from the shell along micromilling trenches following curved growth laminae. The stable isotope values of oxygen ( $\delta^{18}\text{O}$ ) and carbon ( $\delta^{13}\text{C}$ ) from all shell material were measured using an automated carbonate preparation device (KIEL-III) coupled to a gas isotope ratio mass spectrometer (Finnigan MAT 252) at the Environmental Isotope Laboratory, University of Arizona. Powdered samples were reacted with dehydrated phosphoric acid under vacuum at 70  $^\circ\text{C}$ . The isotope ratio measurement is calibrated based on repeated measurements of NBS-19 and NBS-18 and precision is  $\pm 0.10\%$  for  $\delta^{18}\text{O}$  and  $\pm 0.08\%$  for  $\delta^{13}\text{C}$  (1 sigma). The incorporated  $^{17}\text{O}$  correction is that supplied by the ISODAT (ver. 6.2) software. No acid fractionation is applied for the difference between aragonite and calcite. This study focuses on the  $\delta^{18}\text{O}$  results, however the  $\delta^{13}\text{C}$  results are available in [Supplementary Information Table S2](#).

### 2.5. Isotope equilibrium calculations

Freshwater bivalves form their shell material in oxygen isotopic equilibrium with their surrounding water (Dettman et al., 1999; Vonhof et al., 2013). The Dettman et al. (1999) biogenic aragonite fractionation equation is used to calculate the equilibrium oxygen isotope values for the shell ( $\delta^{18}\text{O}_s$ ) and host water ( $\delta^{18}\text{O}_w$ ) at specific temperatures:

$$1000 \ln(\alpha) = 2.559(10^6 T^{-2}) + 0.715 \quad (1)$$

where T is the water temperature in degrees Kelvin and  $\alpha$  is the fractionation between water and aragonite, described by:

$$\alpha = (1000 + \delta^{18}\text{O}_s(\text{VSMOW})) / (1000 + \delta^{18}\text{O}_w(\text{VSMOW})) \quad (2)$$

Note that the aragonite  $\delta^{18}\text{O}$  data reported in both this paper and in Dettman et al. (1999) are calibrated using calcite standards and do not incorporate an aragonite-specific acid-fractionation factor, therefore the



fractionation relationship of eq. (1) is applicable to the shell data reported here. In order to apply equations (1) and (2), the  $\delta^{18}\text{O}_s$  (Vienna PeeDee Belemnite-VPDB) values are converted to  $\delta^{18}\text{O}_s$  (Vienna Standard Mean Ocean Water-VSMOW) values using this relationship (Sharp, 2007):

$$1.03091 = (1000 + \delta^{18}\text{O}_s \text{ (VSMOW)}) / (1000 + \delta^{18}\text{O}_s \text{ (VPDB)}) \quad (3)$$

When applying Equation (1) to fossil shell carbonate precipitated at equilibrium conditions, two environmental variables are not known, water temperature and  $\delta^{18}\text{O}_w$ . Given the Turkana Basin's proximity to the equator and past measurements of the annual cycle of Lake Turkana surface waters, it is expected that seasonal water temperature variation will have only a limited effect on  $\delta^{18}\text{O}_s$  (~1–1.5‰). The range in modern Lake Turkana seasonal open-lake, surface water temperature variation away from river inputs is 25 °C–31 °C, whereas deep water temperature varies between 25.5 °C and 26.5 °C (Ferguson and Harbott, 1972; Yur-etch and Cerling, 1983; Cohen, 1986; Källqvist et al., 1988). The modern Omo River delta is seasonally cooled by river-flood discharge and surface water temperatures near the delta range from 23 °C to 25 °C (Cohen, 1986). The maximum Omo River discharge into Lake Turkana occurs during August and September, with mean monthly maximum discharge ranging from 1506 to 1677 m<sup>3</sup>/s for years between 1964 and 2000 (Ethiopia Electric Power Corporation EEPCCO, 2009). Therefore, in this setting the primary controls on seasonal  $\delta^{18}\text{O}_s$  values and variability are the amount of monsoonal precipitation and dry season evaporation of the lake surface water (Abell et al., 1995; Vonhof et al., 2013). Using this limited temperature range, we calculated the equilibrium  $\delta^{18}\text{O}_w$  value of the ambient water for modern and Late Holocene *E. elliptica* shells and compared those values to the measured  $\delta^{18}\text{O}_w$  of Lake Turkana and Omo River water as an indicator of shell provenance (Vonhof et al., 2013; Ricketts and Johnson, 1996; Cerling et al., 1988; Ng'ang'a et al., 1998; Levin et al., 2009).

Given the previously mentioned considerations, we assume that the variability of  $\delta^{18}\text{O}_s$  within shells of the Omo-Turkana system is primarily controlled by proportional changes in the inflow of river runoff, which has lower (unevaporated)  $\delta^{18}\text{O}$  values, and which mixes with the lake water that has higher isotope ratio values. Thus, the  $\delta^{18}\text{O}$  values in the shells afford us a means for determining the approximate lifespan of these bivalves, the season of death and specific growth increments (given sufficient variability), and the comparative range of variation in this seasonal inflow of river water. This range is most likely tied to the proximity of river water input to the lake system. Note that factors other than runoff amount can affect the  $\delta^{18}\text{O}$  of shell carbonate in this system: changes in the  $\delta^{18}\text{O}$  of the Omo River water, changes in the temperature of either river water or shallow lake water, and variation in local relative humidity all could lead to changes in the evaporation history of shallow lake water and its  $\delta^{18}\text{O}$  value. All of these factors could have an impact on the seasonal cycles in the shells of this study, but for shells of the river/lake mixing zone or in shallow lake shore environments, runoff variability is most likely the dominant feature causing  $\delta^{18}\text{O}$  fluctuations.

## 2.6. Sclerochronology

The periodicity of growth laminae accretion and the relationship between growth laminae accretion with shell stable isotopes was investigated for one of the *E. elliptica* shells, fossil E3. Microscopic images of fossil E3 hinge growth laminae (along the isotopic sampling transect) were taken at 250X using a Leica M165 C microscope. Manual visual layer counting of dark growth lines (de Winter et al., 2020) was performed on the microscopic images of the hinge of fossil E3, the fossil *Etheria* in which the growth bands were most clearly and continuously visible. Profile lines of grayscale value maxima were recorded along the entire length of fossil E3 hinge microscopic images to detect dark growth lines using ImageJ. The visually counted growth lines were compared to ImageJ plot profile line gray value maxima data to address potential

errors in manual visual layer counting. The growth increment width, defined as the distance between two subsequent dark growth lines, was calculated from ImageJ plot profile line data as the distance between gray value maxima on the microscopic images.

To align the stable isotope and growth increment width data, a distance measuring tool was used on microscopic images of the fossil E3 hinge to measure the distance of each stable isotope drill hole along the hinge. This allowed for stable isotope values to be aligned to growth increment width data along the length of the hinge. The average growth increment width across the 0.3 mm micro-drill holes, and the median growth band increment width  $\pm 0.5$  mm around the micro-drill holes, were compared to the  $\delta^{18}\text{O}_s$  data using linear  $r$  (Pearson) values, to investigate whether a correlation exists between growth band increment widths and oxygen isotope values. Such a correlation might exist if growth was favored under increased, nutrient-rich riverine inflow for example, or as a result of changing water temperature, which would also affect oxygen isotopes. A continuous wavelet transform spectral analysis of the growth increment width time series, in comparison to seasonal  $\delta^{18}\text{O}_s$  data, was calculated to investigate *E. elliptica* laminae accretion periodicity. All statistical analyses were performed using PAST 4.03 (Hammer, 2020).

## 2.7. Clumped isotope ratio measurement and paleotemperature estimation

For carbonates, the conventional isotope ratios ( $\delta^{18}\text{O}$ ,  $\delta^{13}\text{C}$ ) and clumped isotope ( $^{13}\text{C}$ - $^{18}\text{O}$  bonds,  $\Delta_{638}$ ) content in excess of a stochastic distribution of isotope combinations were measured using a tunable infrared laser differential spectrometer constructed by Aerodyne Research, Boston. The term  $\Delta_{638}$  is the laser measurement equivalent of  $\Delta_{47}$  in mass spectrometry-based analysis. Complete details of this method and the calibration of the temperature –  $\Delta_{638}$  relationship are described in Yanay et al. (2022). About 2 mg of powdered carbonate is reacted with dehydrated phosphoric acid under vacuum at 70 °C. The  $\delta^{18}\text{O}$  and  $\delta^{13}\text{C}$  measurement relative to VPDB is calibrated based on repeated measurements of International Atomic Energy Agency (IAEA) reference materials (NBS-19 and NBS-18). Clumped isotope values ( $\Delta_{638}$ ) are reported in the CDES (Carbon Dioxide Equilibration Scale) reference frame defined by a comparison of the clumped isotope ratio of water-equilibrated  $\text{CO}_2$  samples with theoretical abundances of clumped species. Clumped results are calibrated based on water-equilibrated  $\text{CO}_2$  gases, heated  $\text{CO}_2$  gases (1000 °C), and ETH 1–4 carbonate standards. The precision for these measurements are  $\pm 0.023\text{‰}$  for  $\Delta_{638}$ ,  $\pm 0.04\text{‰}$  for  $\delta^{18}\text{O}$ , and  $\pm 0.03\text{‰}$  for  $\delta^{13}\text{C}$  (pooled reproducibility, 1-sigma, error propagation method of Daeron, 2021). The laser-based  $\Delta_{638}$  – temperature relationship for carbonates (Yanay et al., 2022) is based on 51 synthetic calcites equilibrated at temperatures from 6 °C to 1100 °C. It is indistinguishable from recent mass spectrometry-based  $\Delta_{47}$  – temperature relationships (e.g. Anderson et al., 2021), and correctly predicted precipitation temperatures for a suite of 17 natural carbonates (both calcite and aragonite) (full details in Yanay et al., 2022). For high precision, replicated, measurements of  $\Delta_{638}$  associated uncertainties in calculated temperature are typically  $\pm 2$ – $3$  °C.

For all clumped isotope measurements we have also calculated the  $\delta^{18}\text{O}$  of the ambient water, based on the temperature derived from  $\Delta_{638}$  and the  $\delta^{18}\text{O}_s$ , as described in Yanay et al. (2022). However, because the relationship in that paper is based on isotope ratios in calcite, an additional calculation of water  $\delta^{18}\text{O}$  values based on the resulting temperatures and  $\delta^{18}\text{O}$  of aragonite shells must be done, using Dettman et al. (1999) for the aragonite-water fractionation system. The measured  $\delta^{18}\text{O}_s$  value and calculated temperature are entered into the aragonite-specific fractionation relationship to calculate ambient water  $\delta^{18}\text{O}$  values.

Clumped isotope data ( $\Delta_{638}$ ) were collected and used to calculate paleotemperatures for a subset of eight of the *Etheria* and *Pseudobovaria* fossils (*E. elliptica* samples Ee79, LobuniEe1, Ee2, Mid-Holocene E2 and E3; *Pseudobovaria* sp. samples 31-32-01, 33-34-02 and 79-80-02).

Several of these fossils had more than one analysis and paleotemperature estimated from different growth positions. For the large *Etheria* shells our strategy was to obtain measurements on samples from the same growth positions for which conventional stable isotope growth series measurements were collected. Furthermore, we measured clumped isotopes at growth positions where prior conventional isotopic measurements showed the greatest seasonal difference in  $\delta^{18}\text{O}_s$ , on the assumption that these might also capture the greatest temperature seasonality. For the smaller *Pseudobovaria* shells from the drill core it was not possible to obtain multiple clumped isotopic measurements within a single shell because of shell mass limitations. Therefore, only bulk measurements of these shells were collected. When possible, all shell samples were measured in triplicate for clumped isotopes, although two samples are only duplicated.

### 3. Results

#### 3.1. Modern and Late Holocene shell conventional stable isotopes

The seasonal  $\delta^{18}\text{O}_s$  data for shells Ee Cohen 79 and Lobuni Ee 1–3 are presented in Fig. 3, Fig. 4 and Table S2. Shell Ee Cohen 79 was alive shortly before collection, based on its ultramodern  $^{14}\text{C}$  age (Table 2), and it displays relatively low  $\delta^{18}\text{O}_s$  values ( $-0.3\text{‰}$  to  $-2.5\text{‰}$  VPDB) through  $\sim 1.5$  years of growth (Fig. 3, growth duration estimated from number of major cycles in the O isotope data). Application of Eq. (1) across a range of surface water temperatures from  $24^\circ\text{C}$  (the average of observed water temperatures for the Omo River delta) to  $30^\circ\text{C}$  (close to the highest temperature observations for open Lake Turkana waters) indicates that the shell could have lived in lake/delta waters (Eq. (2)) with  $\delta^{18}\text{O}_w$  values ranging from  $+1.6\text{‰}$  to  $-1.7\text{‰}$  (VSMOW). Shells Lobuni Ee 1, 2 and 3 are Late Holocene in age ( $\sim 400$ – $500$  cal. yr. BP, Table 2) and individually exhibit a broader range of isotopic variability than the modern shell, with overall more  $\delta^{18}\text{O}_s$  positive values over  $\sim 2.5$  years of growth (Fig. 4). The seasonal  $\delta^{18}\text{O}_s$  range for Lobuni Ee 1 is from  $4.7\text{‰}$  to  $-2.6\text{‰}$  (VPDB) and the range of equilibrium water  $\delta^{18}\text{O}_w$  values calculated for temperatures from  $24^\circ\text{C}$  to  $30^\circ\text{C}$  is  $6.5\text{‰}$  to  $-1.9\text{‰}$  (VSMOW). The seasonal  $\delta^{18}\text{O}_s$  range for Lobuni Ee 2 is from  $4.8\text{‰}$  to  $-2.2\text{‰}$  (VPDB) and the calculated equilibrium  $\delta^{18}\text{O}_w$  range is  $6.7\text{‰}$  to  $-1.5\text{‰}$  (VSMOW). The seasonal  $\delta^{18}\text{O}_s$  range for Lobuni Ee 3 is  $3.3\text{‰}$  to  $-2.0\text{‰}$  (VPDB) and calculated  $\delta^{18}\text{O}_w$  range is  $5.2\text{‰}$  to  $-1.2\text{‰}$  (VSMOW).

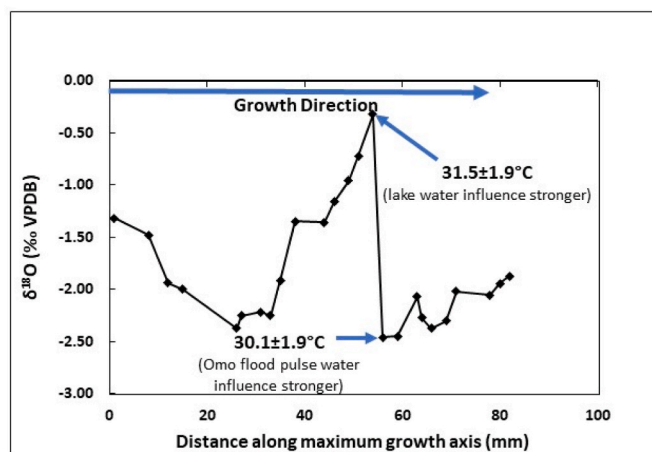


Fig. 3. Oxygen isotope profile of the modern *Etheria elliptica* shell from the Omo River (Ee Cohen 79). Two clumped isotope temperature inferences are marked with arrows.

#### 3.2. Middle Holocene shells

Fossils E2 and E3 are of Middle Holocene age (Table 2) and show less isotopic variability than the modern and Late Holocene *E. elliptica*, with exclusively positive  $\delta^{18}\text{O}_s$  values (Fig. 5a,  $n = 15$  for each of the three shells). Fossil E2 is slightly younger ( $5389 \pm 78$  cal yr. BP), with more positive  $\delta^{18}\text{O}_s$  values and a small seasonal range ( $3.6\text{‰}$ – $3.0\text{‰}$  VPDB). Fossil E3 is several hundred years older ( $5778 \pm 126$ ) than E2, with slightly lower  $\delta^{18}\text{O}_s$  values, and also displays a small seasonal range ( $2.9\text{‰}$ – $2.2\text{‰}$  VPDB). Because both Middle Holocene *E. elliptica* lack a large or clearly defined cyclic seasonal isotopic pattern, the number of years of growth recorded by the shells is uncertain.

The well-preserved *E. elliptica* shells examined in this study contain regular microscopic light-dark growth bands (Fig. 5b and c), averaging  $74 \pm 45 \mu\text{m}$  in width in the E3 shell examined. The sclerochronological growth increment width time series for fossil E3 is presented in Fig. 5b. A total of 404 dark growth lines were counted in microscopic images of fossil E3's hinge. However, this number is likely an underestimate of the originally-produced growth bands as a result of degradation of the fossil hinge surface obscuring growth laminae in some portions of the images. Nevertheless, the total number and size of these bands, when compared with the isotopic evidence for shell growth duration, suggest these may represent diurnal growth increments (Velarde et al., 2015; de Winter et al., 2020). However, for fossil E3 there is no conclusive relationship between growth laminae width and stable isotopes (linear  $r$  (Pearson)  $> 0.05$ , analyzed both for means and median growth band widths), suggesting that possible correlates of seasonal river inflow that would cause stable oxygen isotopes to vary, such as temperature or evaporative enrichment do not strongly influence growth rates. (Fig. S3).

Given the possibility that the light-dark growth increments in the E3 shell are diurnal, we examined the pattern of growth increment thicknesses through the entire growth time-series assuming the micron scale increments are diurnal to see if any other likely drivers of growth increment cyclicity were evident. A continuous wavelet transform spectral analysis of growth increment width data shows episodic peaks in power around periods of  $\sim 7$ – $\sim 14$  increments (= presumed days) (Fig. S2). The 14 band (presumed biweekly) periodicity observed in these data may indicate a lunar influence on *E. elliptica* laminae accretion, as suggested for other lacustrine mollusk growth periodicity by Abell et al. (1995). However, the biological explanation for synodic rhythm bivalve growth in equatorial freshwater settings with extremely small tidal amplitudes is unclear. Additionally, with no temporal constraint on fossil E3 lifespan from seasonal stable isotopes, frequency of growth laminae accretion cannot be determined with any certainty.

#### 3.3. Pleistocene shells

The Raman spectra of two Pleistocene ( $\sim 1.6$  Ma) *Pseudobovaria* sp. shells collected from the WTK13 drill core indicate aragonite mineralogy (Fig. S1), and thus hardly any diagenesis occurred in these samples. The seasonal  $\delta^{18}\text{O}_s$  results for six *Pseudobovaria* sp. shells sampled from the WTK13 31Q-2 core at a depth of 83–85 m below surface are presented in Fig. 6. Overall, these shells exhibit a broad range of isotopic variability over  $\sim 0.5$ – $\sim 3$  years of growth, similar to Late Holocene *E. elliptica* shells (Samples 31-32-01  $n = 41$ ; 33-34-01  $n = 26$ ; 33-34-02  $n = 29$ ; 78-79-01  $n = 28$ ; 79-80-01  $n = 48$ ; 79-80-02  $n = 28$ ). Three *Pseudobovaria* sp. specimens from a shell bed interval at 31–34 cm (Fig. 2c) have seasonal  $\delta^{18}\text{O}_s$  ranges of  $4.2\text{‰}$  to  $-1.1\text{‰}$ ,  $4.7\text{‰}$  to  $-1.4\text{‰}$  and  $3.9\text{‰}$ – $0.6\text{‰}$  (VPDB), respectively (Fig. 6a–c). Three *Pseudobovaria* sp. specimens from a shell bed interval at 78–80 cm (Fig. 2d) have seasonal  $\delta^{18}\text{O}_s$  ranges of  $5.2\text{‰}$  to  $-2.1\text{‰}$ ,  $5.1\text{‰}$  to  $-0.6\text{‰}$  and  $4.3\text{‰}$  to  $-0.1\text{‰}$  (VPDB) (Fig. 6d–f).

#### 3.4. Clumped isotope paleotemperature estimates

Clumped isotope measurements of the 13 analyzed samples ranged

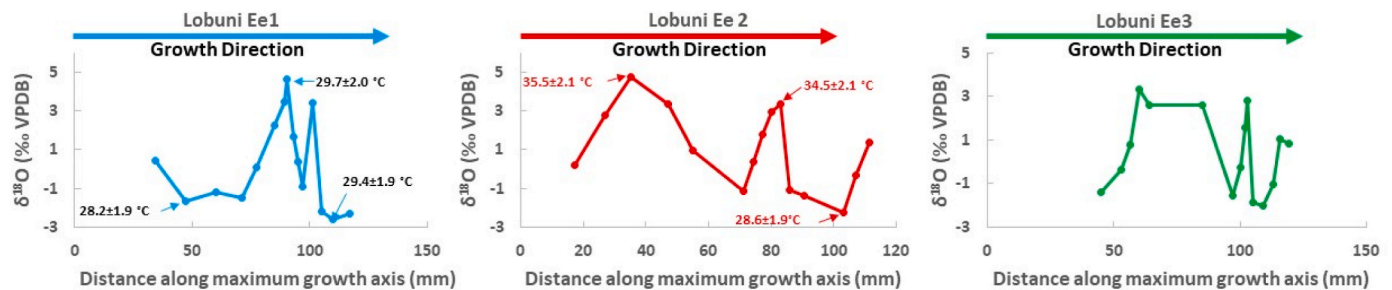


Fig. 4. Oxygen isotope profiles of Late Holocene *Etheria elliptica* shells from the Lobuni Beds, lower Omo River channel. Clumped isotope temperatures are marked on shell sample sequences. See Table 1 for additional sampling location and contextual information.

Table 1

Summary of modern and fossil bivalves and core records discussed in this study.

Taxa	Age	Geologic/Geographic Origin of Fossils (see Fig. 1 for map locations)	Sampling Source of Fossils	Observed/Inferred Environment of Origin	Datasets Analyzed	Data Source
<i>Etheria elliptica</i>	Modern (collected 1979)	Omo R. delta (pre-dam)	Surface collected on small beach	Delta	O and C Isotopes, Clumped Isotopes, $^{14}\text{C}$	This study
<i>E. elliptica</i>	Late Holocene (~400–500 cal yr BP)	Lobuni Beds, lower Omo R. channel	Outcrop	Delta	O and C Isotopes, Clumped Isotopes, $^{14}\text{C}$	This study
<i>E. elliptica</i>	Middle Holocene (~5400–5800 cal yr BP)	Galana Boi Beds, East Turkana Basin	Outcrop	Lake Margin	O and C Isotopes, Clumped Isotopes, $^{14}\text{C}$ , Sclerochronology and time series analysis	This study
<i>Pseudobovaria</i> sp.	Early Pleistocene (~1.63 Ma)	Nachukui Fm, West Turkana	WTK13 Drill Core	Coquina, moderate energy, wave reworked lake deposit, probably littoral-shallow sublittoral	O and C Isotopes, Clumped Isotopes	This study
<i>Iridina omoensis</i> , <i>Pleiodon bentoni</i> , <i>Coelatura</i> sp. and <i>Etheria elliptica</i>	Early Pleistocene (~1.87–1.925 Ma)	Koobi Fora Fm, East Turkana	Outcrop	Lake margin, littoral-shallow sublittoral	O and C Isotopes	Vonhof et al., 2013
N/A	Late Pleistocene-Holocene (~14-0 cal yr BP)	South Basin, Lake Turkana	Composite Piston Core record)		TEX <sub>86</sub> lake temperatures	Morrissey et al., 2018

Table 2

AMS  $^{14}\text{C}$  ages of bivalve mollusk shells from the Turkana Basin. Radiocarbon ages given before Year 1950.  $^{14}\text{C}$  calibration method: OxCal with IntCal20 curve (Reimer et al., 2020). Lab and AA numbers are U. Arizona AMS ID numbers.

Laboratory/AA#	Sample ID	Species	$\delta^{13}\text{C}$ (‰)	Laboratory age (yr BP)	Calendar corrected age (cal yr BP)	Collection location
X36472/AA114867	Ee Cohen 79	<i>Etheria elliptica</i>	-7.3	-2297	post-bomb ultra-modern (1979)	Northwest Turkana near Omo River delta
X36294/AA114691	Lobuni Ee 1	<i>Etheria elliptica</i>	-9.9	443	495.5 ± 35.5	Lobuni Beds, Lower Omo River
X36295/AA114692	Lobuni Ee 2	<i>Etheria elliptica</i>	-5.7	320	385 ± 79	Lobuni Beds, Lower Omo River
X36296/AA114693	Lobuni Ee 3	<i>Etheria elliptica</i>	-10.8	364	405.5 ± 90.5	Lobuni Beds, Lower Omo River
X36297/AA114694	fossil E2	<i>Etheria elliptica</i>	-4.7	4640	5388.5 ± 77.5	Koobi Fora outcrops, Northeast Turkana
X36298/AA114695	fossil E3	<i>Etheria elliptica</i>	-8.1	5022	5778 ± 126	Koobi Fora outcrops, Northeast Turkana

from 0.607 to 0.648 in the CDES reference frame (Table 3, Fig. 3). Calculated ambient water  $\delta^{18}\text{O}_w$  values are listed in Table 3.

The modern (1979) *Etheria* shells yielded temperatures of  $30.1 \pm 1.9$  °C and  $31.5 \pm 1.9$  °C, which are at the upper end of typical modern Omo deltaic water temperature ranges. The warmer temperature measurement is associated with the highest  $\delta^{18}\text{O}_s$  measurement in this shell's growth series. This result is consistent with an interpretation that this shell growth point occurred when this individual was growing in standing (stagnant) lake or deltaic water (calculated  $\delta^{18}\text{O}_w = +1.6$ ‰ VSMOW) immediately prior to the Omo River flood pulse (~May–June 1979). This time of year coincidentally is also the period of warmest open lake surface waters (driven by, but lagging behind local air temperatures because of thermal inertia). In contrast, the sample immediately after this in the growth series yielded a much lower  $\delta^{18}\text{O}_w$  and cooler clumped isotope measurement. This result is consistent with an interpretation that this growth point formed during the part of the year that is coolest from local atmospheric forcing, and also early in the flood

pulse in 1979 (July–September), several months prior to the shell's collection, when cooler Omo River waters, with a  $\delta^{18}\text{O}_w$  value of approximately -0.6‰ (VSMOW), dominated the shell's growth environment (Table 3).

The two Late Holocene Lobuni Beds *Etheria* (Lobuni Ee 1 and Ee 2) shells were each analyzed at three shell growth positions (Fig. 4). These also yielded realistic temperatures in the ~28–30 °C range, except for two anomalously high temperature measurements ( $35.5 \pm 2.1$  and  $34.5 \pm 2.1$  °C), both in shell Lobuni Ee2. Four of the six temperature estimates in these two shells are within error of the others (excluding the 34–36 °C outliers), so it is not possible to observe a pattern in the relationship between  $\delta^{18}\text{O}_s$  and temperature of shell formation, as seen in the modern shell (Fig. 3). For  $\delta^{18}\text{O}_s$  values that suggest either an ambient water derived from the Omo River (-1.5 to -3‰ VPDB; see earlier discussion in Section 2.5 of general drivers of O-isotopic variability) or derived from the more evaporated lake water (+1 to +5‰ VPDB), the temperature of shell growth was very similar. Ambient water calculations based



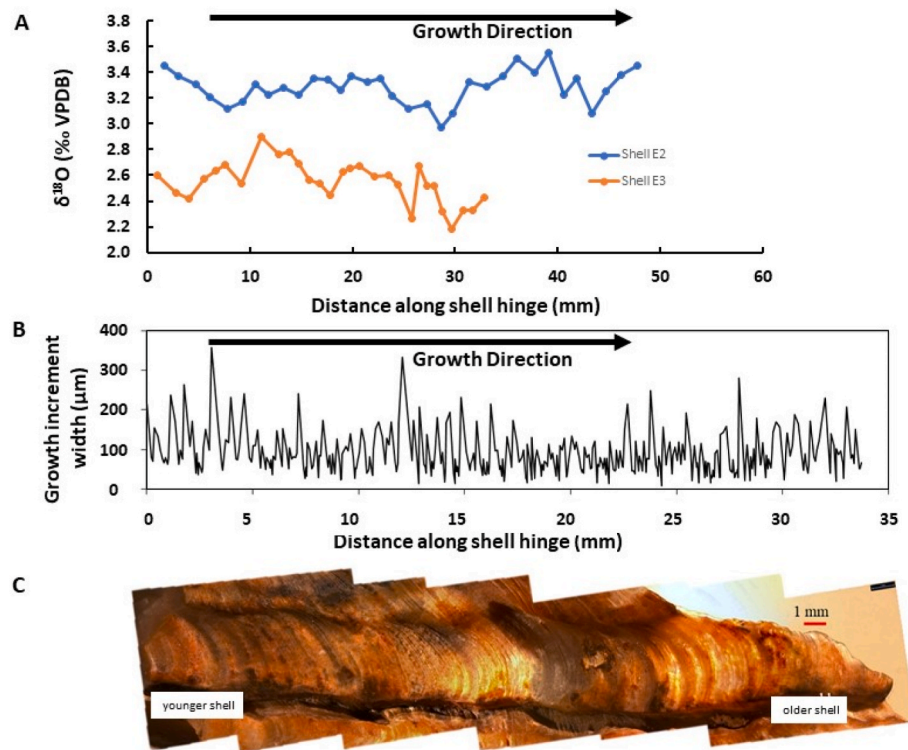


Fig. 5. A. Sclerochronological oxygen isotope profiles for Middle Holocene *Etheria elliptica* shells from Galana Boi Beds. See Table 1 for additional sampling location and contextual information. B. Growth increment width time series of fossil E3 hinge. C. Microscope image of growth laminae along fossil E3 hinge at same scale as panel B.

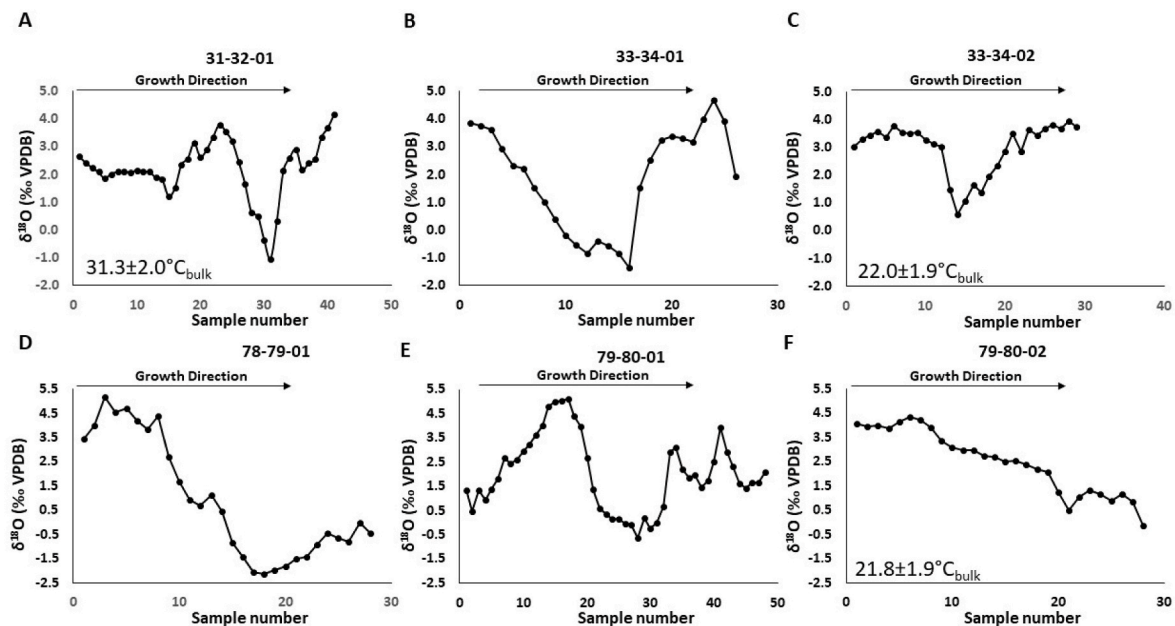


Fig. 6. Sclerochronological oxygen isotope profiles of Pleistocene *Pseudobovaria* sp. shells sampled from the HSPDP WTK13 1A-31Q-2 core. See Table 1 for additional sampling location and contextual information. A-C. Shells from the shell lag interval at 31–34 cm. D-F. Shells from the coquina interval at 78–80 cm. Clumped isotope temperatures are listed in the lower right corner for three shells.

on  $\Delta_{638}$  also imply two competing water sources, Omo River derived with  $\delta^{18}\text{O}$  values of approximately  $-1.0\text{‰}$  (potentially similar to modern values), and Lake Turkana derived with  $\delta^{18}\text{O}$  values of  $+6.4$  to  $+6.9\text{‰}$  (VSMOW - Table 3, slightly above modern mean values). However, there is a strong contrast in the  $\delta^{18}\text{O}$  values measured in these shells, implying a seasonal alternation between the influence of lake

water and of Omo River water at the shells' location, there is no large contrast in the temperature of either water source at this location.

A single sample was drilled across all growth bands for each of the Middle Holocene shells (Fig. 5). The two temperatures calculated from these  $\Delta_{638}$  values ( $29.6 \pm 2.0^\circ\text{C}$  and  $27.2 \pm 2.0^\circ\text{C}$ ) are well within the range of modern Lake Turkana temperatures and consistent with TEX<sub>86</sub>-

**Table 3**

Clumped isotope measurements and paleotemperature estimates. Errors indicated for T in °C indicate the composite 95% confidence interval values, based on pooled variability of carbonate standards run on the laser system and uncertainties inherent in the T calibration (see Yanay et al., 2022). For d18O<sub>w</sub> the indicated errors are dominated by the T uncertainties plus a small contribution from the 1σ uncertainty on shell d18O.

	n	D638	SD	Calculated T °C.	Error T °C	d13C VPDB	d18O VPDB	d18O <sub>w</sub> (calcite based)	d18O <sub>w</sub> (aragonite based)	
'001#EeCohen79Sample17'	3	0.618	0.009	31.5	1.9	-12.87	-0.55	2.84	1.59	0.55
'001#EeCohen79Sample18'	2	0.622	0.021	30.1	1.9	-7.99	-2.50	0.62	-0.62	0.56
'001#LobuniEe1_2'	3	0.628	0.013	28.2	1.9	-9.11	-1.01	1.74	0.53	0.56
'001#LobuniEe1_8'	3	0.624	0.002	29.7	2.0	-7.33	4.69	7.77	6.53	0.57
'001#LobuniEe1_14'	3	0.624	0.016	29.4	1.9	-9.17	-2.80	0.19	-1.04	0.56
'001#LobuniEe2_3'	3	0.607	0.018	35.5	2.1	-7.92	3.99	8.17	6.85	0.57
'001#LobuniEe2_10'	2	0.610	0.003	34.5	2.1	-8.13	3.72	7.72	6.41	0.57
'001#LobuniEe2_13'	3	0.627	0.027	28.6	1.9	-7.82	-2.72	0.10	-1.11	0.56
'001#MidHoloE2bulk'	3	0.624	0.024	29.6	2.0	-4.36	2.60	5.65	4.42	0.57
'001#MidHoloE3bulk'	3	0.631	0.013	27.2	2.0	-2.39	2.49	5.06	3.85	0.58
'001#Pleistocene31-32-01'	3	0.619	0.032	31.3	2.0	-4.13	1.72	5.10	3.85	0.57
'001#Pleistocene33-34-02'	3	0.647	0.015	22.0	1.9	-3.87	2.22	3.71	2.56	0.57
'001#Pleistocene79-80-02'	3	0.648	0.005	21.8	1.9	-2.79	1.45	2.91	1.76	0.57

based estimates (24–29 °C) for mid-lake waters in Lake Turkana during the Middle Holocene, during the rapid termination phase of the African Humid Period when Lake Turkana transitioned from an open to a closed system (Garcin et al., 2012). Calculated water δ<sup>18</sup>O values are between ~3.9 and 4.4‰ (VSMOW - Table 3).

Three of the six Early Pleistocene *Pseudobovaria* shells shown in Fig. 6 were sampled for clumped isotope ratios. Because of the small size of the shells a single bulk sample was taken from each. The resulting temperatures cover a wide range (Fig. 6). As noted previously, *Pseudobovaria* is an extinct genus, and little is known paleoecologically about its optimal habitat range beyond a known occurrence in freshwater (Van Bocxlaer, 2020). The two lower temperatures recorded (22.0 ± 1.9 and 21.8 ± 1.9 °C) are well below modern Lake Turkana temperatures. Calculated δ<sup>18</sup>O<sub>w</sub> values for these two samples are also notably lower than modern Lake Turkana waters, suggesting either increased water input, a less evaporated lake system, or both, all of which are consistent with previous studies demonstrating that at this time the lake had a hydrologic outlet to the Indian Ocean (Feibel, 1994, 2011). Conversely, the high temperature measurement (31.3 ± 2.0 °C) is near the upper end of modern instrumental measurements for Lake Turkana. This sample suggests δ<sup>18</sup>O<sub>w</sub> values slightly below the modern lake (Table 3). The three *Pseudobovaria* shells all come from shell lag beds, which in other large African rift lakes are interpreted as forming as time-averaged assemblages produced as a consequence of lake level fluctuations over time frames of ~10<sup>1</sup>–10<sup>3</sup> years (Cohen, 1989; McGlue et al., 2009; Van Bocxlaer et al., 2012; Soreghan et al., 2021). This is also consistent with the facies analysis of deposits from paleolake Lorenyang within which these shell beds occur, which indicate repeated, high frequency lake level fluctuations (Beck et al., 2015). It is possible that Paleolake Lorenyang experienced much greater seasonal or vertical water temperature variability during the early Pleistocene (~1.6 Ma) than modern Lake Turkana (i.e. ~9–10 °C combined vertical and seasonal temperature range for Paleolake Lorenyang at ~1.6 Ma, vs. ~6 °C in Lake Turkana today), or alternatively that the time averaging for shells within these lag deposits has admixed shells formed under substantially different climate regimes.

## 4. Discussion

### 4.1. Modern and Late Holocene samples

Stable oxygen isotope values of shell growth laminae reflect the host water environment in which they grew. The amplitude of δ<sup>18</sup>O<sub>s</sub> in different shells can be used to investigate seasonal hydroclimate variability across time. Such studies are particularly useful for deltaic shells which display highly contrasting seasonality between lake and river water and uniquely allow for interpretation of both local (Lake Turkana) and upstream (Ethiopian Highlands) hydroclimate. The most positive

δ<sup>18</sup>O values could have been produced in shells that were growing in the lake proper under conditions of increased evaporation, or alternatively in areas of the delta temporarily cut off from river flow resulting in partial desiccation, whereas the most negative δ<sup>18</sup>O values indicate that growth predominantly occurred when the bivalve was immersed in runoff coming from upstream precipitation over the Ethiopian Highlands. Comparing the isotopic ranges of “modern” (i.e. pre-dam) shells provides us with a benchmark for qualitative paleoenvironmental comparisons.

The calculated δ<sup>18</sup>O<sub>w</sub> for modern and Late Holocene *E. elliptica* shells can be compared to modern measured δ<sup>18</sup>O<sub>w</sub> values from the Omo River and Lake Turkana to constrain the shells' provenance. The exact collection location of shells Lobuni Ee 1–3 is unknown, but described in field notes as the Lower Omo River valley. Shell Cohen Ee 79 has precise collection information (southwest of the Omo River delta) but could have been transported post-mortem an unknown distance downstream along the Omo River towards the lake shore, although its fresh appearance coupled with an ultramodern (~1979) <sup>14</sup>C age argue against a significant lag time between growth and collection. If the δ<sup>18</sup>O<sub>w</sub> values for the water in which the modern shell Cohen Ee 79 lived is calculated, the δ<sup>18</sup>O<sub>w</sub> values range from -0.6‰ (VSMOW) to +1.6‰ (Table 3), values that are either within the range of measured Omo River water values, or that imply a mixture of lake and river water (Ricketts and Johnson, 1996; Ng'ang'a et al., 1998; Levin et al., 2009; Vonhof et al., 2013). Despite being collected along the northwestern shore of Lake Turkana, these calculated δ<sup>18</sup>O<sub>w</sub> values and limited seasonal isotopic variability strongly suggests an Omo River provenance. This shell has δ<sup>18</sup>O<sub>s</sub> values comparable to a modern *E. elliptica* from the Omo River (Vonhof et al., 2013 and Fig. 7c).

Late Holocene shells Lobuni Ee 1–3 exhibit broader seasonal isotopic variability with both positive and negative δ<sup>18</sup>O<sub>s</sub> values. Several of the calculated δ<sup>18</sup>O<sub>w</sub> values that fall in the -1.1 to 0.5‰ (VSMOW) range are comparable to the range of measured modern Omo River water values (-1.2 to -0.1‰, Ricketts and Johnson, 1996), but we also observed values greater than 6‰ (VSMOW), which are within the range of measured Lake Turkana water (+4.4 to +7.2‰ (VSMOW); Ricketts and Johnson, 1996; Ng'ang'a et al., 1998; Cerling et al., 1988; Levin et al., 2009; Vonhof et al., 2013). It is important to note however, that modern values above +6.4‰ (VSMOW) have only been observed in embayments with restricted connectivity to the lake proper (e.g., Ferguson's Gulf, Vonhof et al., 2013). The high amplitudes in δ<sup>18</sup>O<sub>s</sub> values and the resulting range of ambient water δ<sup>18</sup>O<sub>w</sub> values suggest that these Late Holocene *E. elliptica* grew in a mixing zone of Omo River and Lake Turkana waters, where negative δ<sup>18</sup>O<sub>w</sub> values correspond to high Omo River runoff during late boreal summer, coeval with Ethiopian Highland monsoonal precipitation and Omo flood discharge. The much more positive δ<sup>18</sup>O<sub>w</sub> values, greater than 6‰ (VSMOW), could then correspond with either highly evaporated lake water during times of reduced

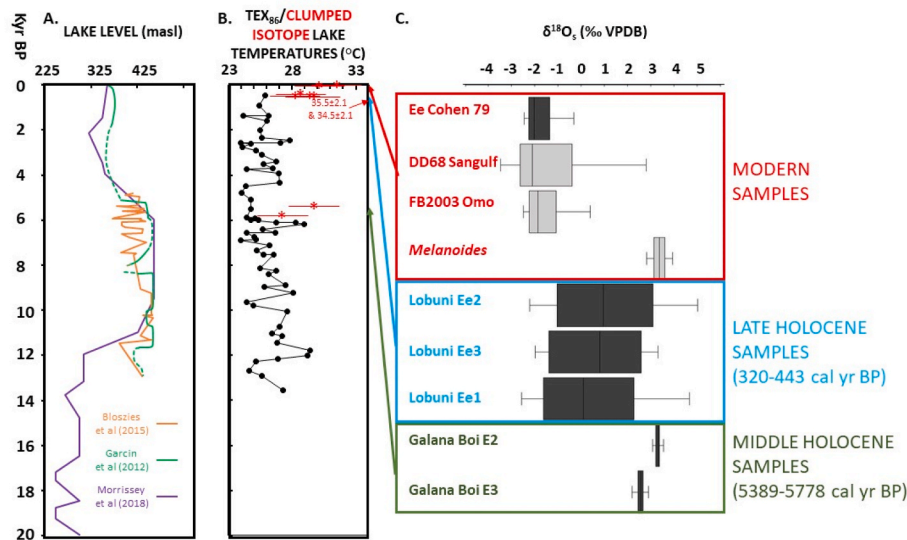


**Fig. 7.** A. Reconstructed lake level for Lake Turkana (m above sea level) using sediment core and seismic reflection data (purple; [Morrissey and Scholz, 2014](#)) and two outcrop-based lake level chronologies. The first is reconstructed from radiocarbon-dated mollusks and optically stimulated luminescence (OSL) quartz grains from relic beach deposits (orange; [Bloeszies et al., 2015](#)), whereas the second represents a more conservative, radiocarbon-based summary interpretation with fewer high-frequency lake-level excursions during the Early-Middle Holocene transition to lower lake levels (green; [Garcin et al., 2012](#)). D. B. TEX<sub>86</sub> lake temperature record for Lake Turkana ([Morrissey et al., 2018](#)) reflecting South Basin metalimnetic/deeper water temperatures (black line/circles) and clumped isotope temperatures, reflecting North Basin surface water temperatures (red asterisks). C. Oxygen isotope ranges of modern and Holocene mollusks from this study (dark gray) and [Vonhof et al. \(2013\)](#) in light gray with corresponding sample IDs. Isotope data are plotted as box and whisker diagrams (showing median, upper and lower quartile, and minimum and maximum isotope values of each specimen studied).

Omo River discharge, or growth in a distributary of the Omo or embayment, which has temporarily become detached from the river's discharge channels, allowing both isotopic enrichment of  $^{18}\text{O}$  through evaporation and increased temperature variability. The broad seasonal isotopic variability indicates a deltaic provenance for shells Lobuni Ee 1–3, with  $\delta^{18}\text{O}_s$  values comparable to a modern Omo River delta mollusc ([Fig. 7a](#)) analyzed by [Vonhof et al. \(2013\)](#).

Late Holocene shells Lobuni Ee 1 and 2 both exhibit a larger seasonal  $\delta^{18}\text{O}_s$  amplitude ( $\sim 7\%$  VPDB) than Lobuni Ee 3 ( $\sim 5\%$  VPDB; [Figs. 4 and 7](#)), consistent with growth under more variable hydroclimate conditions in a closed-basin setting. Specifically, Lobuni Ee 1 and 2 may have grown under more intense Omo River runoff during the late summer (indicated by low minimum  $\delta^{18}\text{O}_s$  values  $< -2\%$  VPDB; [Fig. 4](#)) and exposure to the more evaporative conditions of Lake Turkana for the remainder of the year during base flow conditions. Whereas it is possible that Lobuni Ee 1 and 2 grew during years of enhanced East African monsoon precipitation over Ethiopia as suggested by stronger Omo River runoff, the lake water end-member seems to be much more evaporative at this point in the record. The most positive  $\delta^{18}\text{O}_w$  values derived from any shells in this study are from these two shells (calculated water  $\delta^{18}\text{O}$  values of  $+6.5$  and  $+6.9\%$  VSMOW, [Table 3](#)). This suggests that either Late Holocene lake waters were slightly more evaporated than the modern Lake Turkana, or that these bivalves grew in a backwater channel that was temporarily detached from main Omo River flow and underwent some degree of evaporative isotopic enrichment. As noted previously, evaporative enrichment beyond that of the open waters of Lake Turkana is, in fact, observed in isolated shallow bays today, where temperature extremes and increased evaporation can occur (e.g., [Ferguson's Gulf, Vonhof et al., 2013](#)). Lobuni Ee 3 appears to have grown under less evaporative conditions/fresher water from fall to early summer, indicated by lower maximum  $\delta^{18}\text{O}_s$  values ( $+2.8$ – $3.1\%$ , [Fig. 4](#)). Increased Omo River discharge, or changes in moisture sources to ones with more depleted initial  $\delta^{18}\text{O}$  values could have also leveraged this type of lowered maximum  $\delta^{18}\text{O}_s$  (e.g., [Levin et al., 2009](#)). Short-term, lower evaporation over Lake Turkana during Lobuni Ee 3's lifespan may be attributed to increased cloud cover, higher humidity and/or lower surface air temperatures. As indicated by lake level reconstructions ([Garcin et al., 2012](#); [Bloeszies et al., 2015](#)), regional drying at the termination of the AHP caused the lake level to drop below the basin's northwestern spillway point in the Early-Middle Holocene transition. Subsequently, the lake transitioned to its modern endorheic configuration ( $\sim 330$ – $360$  m.a.s.l.) by the Late Holocene ([Fig. 7a](#)).

#### 4.2. Middle Holocene African Humid Period samples

The AHP was characterized by wetter conditions and higher lake levels across northern hemisphere tropical Africa from 14 to 5 cal yr ka ([Street and Grove, 1979](#)) relative to modern. During the wettest intervals of the AHP, Turkana was a large, deep freshwater lake ( $>22,500$  km<sup>2</sup>) which overflowed northwest into the White Nile drainage ([Butzer and Thurber, 1969](#); [Garcin et al., 2012](#); [van der Lubbe et al., 2017](#)). TEX<sub>86</sub> lake water temperature records from various lakes, including Turkana, indicate that the latter part of the AHP ( $\sim 5$  ka, comparable to our Middle Holocene samples) was also somewhat warmer than present throughout much of eastern Africa ([Morrissey et al., 2018](#)). Lake Turkana was hydrologically connected to Suguta, Kenya to the south and the Ethiopian Highlands to the north during the AHP ([Junginger and Trauth, 2013](#); [Junginger et al., 2014](#); [van der Lubbe et al., 2017](#); [Fischer et al., 2020](#)). As such, the proportion of Omo River input to the lake declined as overflow from Suguta and Chew Bahir lakes plus Kerio River and Turkwel River runoff increased. These additional freshwater inputs filled Lake Turkana to its overflow level and lowered the  $\delta^{18}\text{O}$  values of the water and thus those of calcium carbonate shell-producing organisms living in the lake. As the lake level decreased during the Late Holocene, Turkana transitioned from meromictic to well-mixed and oxygenated at the bottom. Sediment core records from the southern basin of Lake Turkana demonstrate declining organic carbon, increasing total inorganic carbon (TIC) and a shift from laminated organic-rich muds to bedded diatomaceous silt after the AHP ([Morrissey and Scholz, 2014](#)). These records suggest increasing pH and sediment bioturbation as lake level declined. Strong diurnal winds over Lake Turkana increasingly mixed the shallower water column, resulting in decreased lake stratification and increased hypolimnetic oxygen as is presently observed in the lake ([Johnson and Malala, 2009](#)).

Our study provides proof-of-concept work to document the potential of obtaining a completely independent source of lake water temperatures using clumped isotopes besides existing reconstructions using the TEX<sub>86</sub> organic geochemical method ([Schouten et al., 2002](#)). We acknowledge that for both TEX<sub>86</sub> and clumped isotope paleothermometry considerable uncertainties still exist. These include both appropriate temperature calibrations (uncertainties of  $\sim \pm 2$ – $3$  °C) and the inherent standard errors (e.g., mean reproducibility on the order of 1–2 °C for clumped isotopes using the TILDAS method) that accrue from both types of measurements ([Yanay et al., 2022](#); [Kim et al., 2010](#)). But, because both of these problems are likely to diminish in the future and



because these two paleothermometers record different components of a lake's water column, comparisons of contemporaneous data sets using the two methods is warranted. TEX<sub>86</sub> data appear to record temperatures near the base of the mixing zone in tropical lakes, where the Thaumarchaeota microbes produce their membrane lipids (Kraemer et al., 2015), which is typically several degrees cooler than surface waters in the tropics. In contrast, clumped isotopes from mollusks could reflect temperatures at various positions in the water column, but in the case of *E. elliptica*, this would be at or very close to the surface. Thus, a comparison of two contemporaneous data sets holds the potential for reconstructing vertical thermal profile differences in a lake's water column, and this potential will likely improve as the calibration and reproducibility of both methods continue to improve.

Lake Turkana temperatures reconstructed from TEX<sub>86</sub> indicate 0.5 °C mean cooling from the Early Holocene to Late Holocene (Fig. 7b; Morrissey et al., 2018). Notably, our clumped isotope measurements of shallow-water *Etheria* shells do not indicate a significant difference between Middle and Late Holocene surface water temperatures for most of the measurements (although note the two anomalous ~34–35 °C Middle Holocene measurements plus the fact that the imprecision of temperature calculations precludes detection of small differences). Middle-Late Holocene lake deeper water (mixocline) temperatures based on TEX<sub>86</sub> (~25–26 °C) coupled with surface water clumped isotope temperatures from the *Etheria* of the same age range suggest a vertical thermal difference in the lake during much of the Holocene that is similar to that found in current instrumental depth profile data. This observation suggests that the higher Middle Holocene clumped isotope temperature values may reflect growth in isolated water bodies rather than open lake conditions. In contrast to our modern and Late Holocene *E. elliptica* shells, Middle Holocene fossils E2 and E3 have limited isotopic variability (<1‰ VPDB seasonal amplitude) and exclusively positive values that are less than the maximum δ<sup>18</sup>O<sub>s</sub> values from Late Holocene Omo River delta (Lobuni) shells (Fig. 7c). The lower δ<sup>18</sup>O<sub>s</sub> values of the E2 and E3 shells suggest growth during the Middle Holocene in lake water with a positive δ<sup>18</sup>O<sub>w</sub> value, but in fresher, less evaporative conditions than exist today, which agrees with calculated δ<sup>18</sup>O<sub>w</sub> values of 4.4 and 3.9‰ (VSMOW). The δ<sup>18</sup>O<sub>s</sub> seasonality is likely controlled by seasonal freshwater inputs to the lake and may represent a dampened influence of Omo River water, Chew Bahir and/or Suguta overflow into Lake Turkana or Kerio and Turkwel River runoff. However, given that a 1‰ shift in δ<sup>18</sup>O<sub>s</sub> can be driven by a 5 °C temperature change, the limited range of δ<sup>18</sup>O<sub>s</sub> seasonality may in part also be driven by seasonal temperature fluctuations affecting shallow waters near the lake shore.

Middle Holocene fossils E2 and E3 were collected ~10 km north of the Il Bakate, a currently seasonal channel that does not contribute much water to Lake Turkana, but which drained paleolake Chew Bahir to the northeast into Lake Turkana during the AHP. Strontium isotope data (van der Lubbe et al., 2017) and hydrologic provenance modeling (Fischer et al., 2020) indicate that the overflow of Chew Bahir into Lake Turkana ceased by 6 ka. Radiocarbon-dated lacustrine sediments, paleo-shorelines and hydro-balance modeling indicates that the last highstand at paleolake Suguta in the south, and subsequent overflow into Lake Turkana, occurred by 6.5 ka (Junginger and Trauth, 2013; Junginger et al., 2014). After 6 ka, the only major and perennial flows into Lake Turkana would have been the Omo, Turkwel and Kerio rivers. Accordingly, since fossils E2 and E3 are significantly younger than 6 ka, they would have been growing exclusively under the influence of lake waters plus perhaps minor localized groundwater seepage, and δ<sup>18</sup>O<sub>s</sub> values would not have been influenced by paleolake Chew Bahir overflow. Therefore, variations in Omo River runoff, combined with seasonal lake surface water temperature fluctuations are the most likely influences on seasonal δ<sup>18</sup>O<sub>s</sub> values. Thus, the small seasonal amplitude of δ<sup>18</sup>O<sub>s</sub> in bivalves from the Il Bakate area may be attributed to a longer distance to the Omo, Kerio and Turkwel River deltas, and more limited seasonal near-surface water temperature variation <5 °C. Since fossils E2 and E3 did not grow in the Omo River delta, the change in amplitude

of riverine hydrologic seasonality from the Middle to Late Holocene cannot be directly compared, although isotopic variability at this site is perhaps indicative of the Omo seasonal flood influence, even 50 km from its delta.

As a desert lake, Turkana is particularly sensitive to hydroclimate changes with lake level transgressions/regressions of tens of meters occurring on decadal to centennial timescales. It is well established that Lake Turkana expanded in size and depth at the beginning of the Holocene (Garcin et al., 2012), but the timing of regression to the lowstand at the end of the AHP is subject to debate. Paleo-shorelines, sediment core records and seismic reflection data suggest a prolonged highstand throughout the AHP, with lake level falling rapidly after 6 ka (Garcin et al., 2012; Morrissey and Scholz, 2014). Sustained high total sedimentary organic carbon, extremely low total inorganic carbon and continuous flat seismic reflectors from the lake's southern basin indicate calcium carbonate undersaturation (probably low conductivity water), water column stratification and an undisturbed deep-water environment that persisted from the Early Holocene until at least 6 ka, with the lake reaching lower, near-modern levels by ~4 ka (Fig. 7a). However, radiocarbon-dated mollusks and optically stimulated luminescence (OSL) quartz grains from relic beach deposits indicate a more variable lake level history for Turkana during the AHP (Fig. 7a). Forman et al. (2014) identified four major lake level fluctuations >50 m between 8.5 and 4.5 ka during the transition from the AHP to Late Holocene aridity, whereas Bloszies et al. (2015) found up to nine potential lake level fluctuations >30 m between 15 and 4 ka. Both studies indicated a pronounced lowstand at 6 ka and a subsequent highstand at ~5 ka followed by a rapid regression during the termination of the AHP.

Fossils E2 and E3 are dated between 5 and 6 ka, an interval during which Lake Turkana water levels continue to be debated (Fig. 7a). Given the uncertainty surrounding the nature and precise variability of the transition out of the AHP we frame our new data against both the Bloszies et al. (2015) reconstruction, as well as the more conservative (i. e., fewer fluctuations during the ~8–5 ka transition) reconstruction of Garcin et al. (2012). Whereas the shells were collected at 403 m elevation above sea level, it is possible that the lake level during fossils' E2 and E3 lifetimes was several meters above the level of deposition. Slightly more positive lake water δ<sup>18</sup>O<sub>w</sub> values derived from the younger fossil E2 (4.4‰ VSMOW) compared to fossil E3 (3.9‰ VSMOW) suggest that E2 grew in more evaporative lake water. These results may document a transition from fresher water to a more evaporative lake between ~5.9 and ~5.3 ka. Whereas these results could be interpreted as supporting ongoing lake level regression after 6 ka (Garcin et al., 2012; Morrissey and Scholz, 2014), the issue remains inconclusive because the uncertainties in water δ<sup>18</sup>O values derived from the clumped isotope measurement are ~0.6‰, so that both water δ<sup>18</sup>O values are not significantly different. A trend to markedly more evaporative conditions is contradicted by the fact that the two shells were collected from the same elevation, despite being several hundred years different in age. Both the ages and elevations of these *E. elliptica* seem consistent with the lake level model from ~6 to 5 ka of Bloszies et al. (2015), albeit requiring a stabilization in lake levels at ~400 m.a.s.l. between ~5.8–5.4 ka. Age control uncertainties (especially ones related to uncertain old <sup>14</sup>C reservoir effects) may also be contributing to inconsistent Holocene lake-level reconstructions at this level of resolution. It is noteworthy however that the Middle Holocene shells, which individually display relatively low levels of isotopic variability at the seasonal time scale, were growing during a period of relatively strong climate variability at century to millennial time scales, as inferred from both the Garcin et al. (2012) and Bloszies et al. (2015) studies.

The Lake Turkana TEX<sub>86</sub> record collected from the southern basin of Lake Turkana, exhibits a long-term temperature decrease with higher amplitude and higher-frequency variability throughout the AHP (Fig. 7b). As noted previously, TEX<sub>86</sub> temperatures reflect ambient growth temperature of the Thaumarchaeota, living probably in lower O<sub>2</sub> environment (metalimnion) well below the surface (Kraemer et al.,

2015), and thus being buffered from short-term surface water temperature fluctuations. From the Early to Middle Holocene, the mean temperature decreased 1.2 °C (Morrissey et al., 2018), but with considerable scatter in the total range of lake temperatures (5.4 °C) recorded throughout this interval (Fig. 7b). The lake temperature fluctuates within one standard deviation of the mean (25.9 ± 1.1 °C) on a centennial scale for most of the record, with marked increases >28 °C at ~11.7 and ~6.5 ka that are greater than two standard deviations above the mean (Morrissey et al., 2018). Cooler temperatures <25 °C occurred at the end of the AHP between 5.8 and 4.5 ka, during the lifespan of fossils E2 and E3. TEX<sub>86</sub> temperatures at Lake Turkana may be influenced by fluctuations in the wind and waves, mechanical heat transfer and lake mixing (Morrissey et al., 2018). Warmer surface temperatures are often associated in deep tropical lakes with stronger water column stratification (Cohen et al., 2016b), which is consistent with higher lake levels for Lake Turkana for much of the AHP, whereas cooler temperatures associated with greater vertical mixing may have prevailed as lake levels declined during the Middle Holocene. The combination of surface water growth temperatures similar to modern as recorded by the clumped isotopes, coupled with also near modern deeper water temperatures recorded by the TEX<sub>86</sub> data, suggests that the vertical thermal gradient in Lake Turkana during the Middle-Late Holocene (3–5 °C) was comparable to that of today. However, this finding must be tempered by possible thermal differences between the south basin, where the TEX<sub>86</sub> record was derived, and the north basin, where our shell samples were collected.

#### 4.3. Early Pleistocene shells

Early Pleistocene *Pseudobovaria* sp. shells from the WTK13 sediment core exhibit a large seasonal amplitude of  $\delta^{18}\text{O}_s$  (~5–7‰ VPDB, Fig. 6). Based on greenish sediment colors and low TOC values throughout the Paleolake Lorenyang deposits in the drill core (spanning ~1.9–1.4 Ma, Lupien et al., 2018), the lake floor at the drill site appears to have been well oxygenated throughout most or all of this time period. The broad isotopic variability of Early Pleistocene shells is within the range of Late Holocene *E. elliptica*  $\delta^{18}\text{O}_s$  values (Figs. 7c and 8b), but is striking considering the much greater distance from the current Omo Delta position, as well as the inferred fully lacustrine habitat of *Pseudobovaria* sp. (in contrast with the lake margin/fluviol habitat typical of *E. elliptica*). This similarity in  $\delta^{18}\text{O}_s$  values is consistent with several (not mutually exclusive) possible scenarios: 1) A highly seasonal Omo River discharge occurred into paleolake Lorenyang ~1.6 Ma; 2) that this inflow may have exceeded that of the modern Omo River discharge; 3) the Omo inlet was closer to the WTK13 site at ~1.6 Ma than it is today,

or 4) a different source of river water with a low  $\delta^{18}\text{O}_w$  value may have been discharging into Paleolake Lorenyang at this time (e.g., Nutz et al., 2020). Interestingly, two of the three clumped isotope samples from this interval yielded growth temperatures (21.8 and 22.0 °C, on two separate shells) considerably lower than modern lake bottom water temperatures (~24.5–26.0 °C), whereas the third (31.3 °C) is at the upper end of the modern surface water temperature range (~31 °C). It is important to note that we do not know the water depth range that the now-extinct *Pseudobovaria* lived in, although extant members of *Coelaturini* (the tribe to which *Pseudobovaria* likely belongs) occur predominantly in shallow waters (Ortiz-Sepulveda et al., 2020). A nearshore environment is also consistent with the facies analysis of the core segment from which the *Pseudobovaria* shells were retrieved. Thus, on face value, the limited set of clumped isotope temperatures suggest a wider range of temperatures in surface or near surface water at ~1.6 Ma than occurs in Lake Turkana today. The low temperatures indicated in two shells are particularly noteworthy in light of clumped isotope paleotemperature estimates from the same period and location but which were taken from paleosol carbonates, and which suggest ambient temperatures at or considerably above modern values (Passey et al., 2010).

A comparison of the *Pseudobovaria* sp.  $\delta^{18}\text{O}_s$  results with data from slightly older bivalves (a mix of *Iridina omoensis*, *Pleiodon bentoni*, *Coelatura* sp. and *Etheria elliptica*, all between ~1.87–1.925 Ma) from the Koobi Fora Formation (Vanhof et al., 2013) is informative (Fig. 8). The Koobi Fora samples were also collected at a considerable distance from the modern Omo River (~60 km, vs. about 45 km for the WTK drill site) and even further from the paleo-Omo delta location (Brown and Feibel, 1991). However, one of the ~1.9 Ma shells (KJ04-28) was inferred to be deltaic in origin and found to exhibit a narrow seasonal  $\delta^{18}\text{O}_s$  range with negative values only. This shell may have grown under the influence of paleo-river runoff east of the lake (not the Omo River) close to the Koobi Fora area at this time (Fig. 8a). The remaining early Pleistocene Koobi Fora Formation shells, all of which were inferred to be lacustrine, display consistently narrower ranges and more positive  $\delta^{18}\text{O}_s$  values than those from the lacustrine drill core samples from 1.6 Ma. The larger range in seasonal  $\delta^{18}\text{O}_s$  values from our present study may suggest increased seasonal hydrological variability in Paleolake Lorenyang at ~1.6 Ma as compared to ~1.9 Ma. Note, however, that we lack clumped isotope paleotemperature data for the older shells, and thus cannot determine the extent to which this comparison might have been affected by changing temperature variability over that time.

In contrast to the other five Early Pleistocene *Pseudobovaria* shells analyzed, shell 33-34-02 exhibits a smaller seasonal amplitude of  $\delta^{18}\text{O}_s$  (3.5‰ VPDB, Figs. 6c and 8b) with positive values only. The core lithology may explain the different isotopic signatures of shells from the

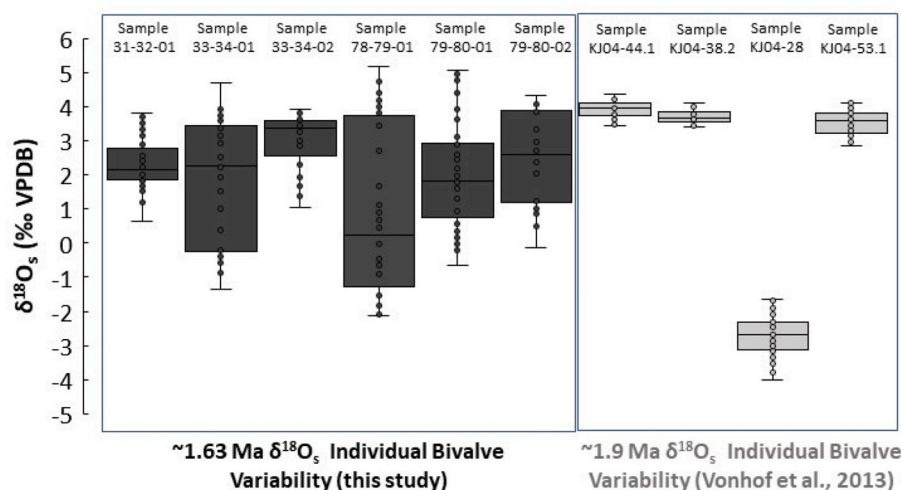


**Fig. 8.** Isotopic variability in Pleistocene shells from Paleolake Lorenyang and their environmental context. Oxygen isotope ranges of Early Pleistocene bivalves obtained from deposits of ~1.9 Ma from the Koobi Fora Fm. east of Lake Turkana (Vanhof et al., 2013) and the ~1.63 Ma specimens from the WTK13 drill core with corresponding sample IDs. Species identifications for individual specimens from Vanhof et al. (2013): KJ04-44.1 = *Coelatura* sp.; KJ04-38.2 and KJ04-28 = *Iridina omoensis*; KJ04-53.1 = *Pleiodon bentoni*. See Fig. 1 for locations. Isotope data are plotted as box and whisker diagrams summarizing the data obtained at different growth positions for each studied specimen, showing means (x) median (mid-line), upper and lower quartile values.

same interval: a shell lag is observed with increasing concentrations of shells and sand up core, followed by an abrupt transition to dark fine-grained sediments (Fig. 2c). An increasing concentration of shells and sand is indicative of falling lake level, whereas abrupt transitions to laminated mud lithologies above the shelly horizons sampled is indicative of a rapid transition to a deeper water environment and lake level rise. As the lake level falls, mud-winning and wave reworking could have mixed the sediments, resulting in shells of different ages being deposited in the same core interval (Cohen, 1989). Analogous to modern-day Sanderson's Gulf at Lake Turkana, the depositional environment of the WTK13 core site during this part of the Early Pleistocene was a lacustrine flat embayment, which is sensitive to lake level fluctuations. As such it experienced many episodes of transgression/regression cycles on varying time scales (Beck et al., 2015). The large cycles in  $\delta^{18}\text{O}_s$  of the five remaining shells strongly suggests that variation in runoff into the lake led to cycles of freshening and evaporation, perhaps associated with these transgressive/regressive cycles. These results may imply a strong wet/dry seasonality at this time. Comparing our data with those of Vonhof et al. (2013) from ~1.9 Ma shells that are strictly lacustrine in nature indicates that even the exclusively positive  $\delta^{18}\text{O}_s$  values of shell 33-34-02 are broader in range (Fig. 8). This comparison suggests that our *Pseudobovaria* sp. experienced different hydroclimate conditions, such as reduced Omo River runoff from lower monsoonal precipitation, or a change in moisture source, during a different time than the other shells from this core interval.

Plio-Pleistocene climate variability in eastern Africa has previously been investigated through paleorecords of changes in lake level, vegetation type and geochemistry. Pollen assemblages (Bonnefille and Umer, 1994), charcoal fluxes and relative proportions of C3 vs C4 vegetation types (Huang et al., 1999; Ficken et al., 2002; Levin, 2015) indicate that vegetation responds to environmental change at time scales much shorter than orbital forcing. High resolution sediment core records provide insight on sub-orbital scale climate variations that impact lake level. The  $\delta\text{D}$  of leaf waxes in the WTK13 paleolake Lorenyang core indicates high-amplitude abrupt hydroclimate changes associated with variations in mean June–August insolation at 20°N, with increased precipitation during high insolation and aridity during low insolation (Lupien et al., 2018, 2020). However, most of these records do not provide direct information on seasonality. In the Turkana Basin, seasonal Omo River runoff from monsoonal precipitation over the Ethiopian Highlands controls modern lake levels (Joordens et al., 2011). Nutz et al. (2020) conclude that paleolake level fluctuations are closely associated with changes in Omo River Valley woody cover, which are indirectly related to seasonally-variable precipitation changes over the Ethiopian Highlands. The use of sclerochronology by Vonhof et al. (2013) and in our study illustrates the contribution of the Omo River flooding cycle and seasonal discharge variation to overall lake hydrologic variability during the Early Pleistocene. Today, and most likely throughout the Pleistocene, the largest contributor to both seasonal and sub-decadal variation (e.g., via ENSO) in Lake Turkana's annual oscillations of lake level, associated water chemistry, and productivity regime is the rainfall-driven flood pulse originating in the distant (400–600 km north) and much wetter Ethiopian Highlands (Ferguson and Harbott, 1972). Variability in precipitation during the Early Pleistocene, and specifically the wet-dry seasonality in the Ethiopian Highlands, appears to have been greater at 1.6 Ma than at 1.9 Ma. Furthermore, combining clumped isotope paleotemperature estimates from nearshore *E. elliptica* with  $\text{TEX}_{86}$ -based records of temperatures at the base of the water column mixing zone provides a new approach to estimating total water column temperature range, and our data suggest that for much of the Holocene, this range was comparable to present. In contrast, our clumped isotope paleotemperature data suggest lake temperatures may have been both more variable and cooler at ~1.6 Ma than at present. This finding about Early Pleistocene lake temperatures however must still be tempered by our uncertainty about the water

depth at which the extinct *Pseudobovaria* lived as well as the thermal structure of the water column at that time.

The data sets we have presented in this paper only provide “snapshots” of seasonal to subdecadal changes in Omo River discharge (and thus indirectly of precipitation fluctuations through the several annual cycles registered in individual bivalve growth records) coupled with limited quantitative temperature reconstructions over the same intervals. However, we see this approach as a very promising “proof-of-concept” demonstration of how reconstructions of precipitation and temperature variability over short time scales can be combined to obtain insight in vertical variation in water properties, and, therefore, potentially in mixing regimes. In future studies, combining these two types of proxy data (precipitation and temperature) in more extensive paleorecords could allow a more complete understanding of both past water availability and heat in driving metabolic stresses on aquatic and terrestrial organisms over their life spans, and it may provide insight into paleolimnological drivers of lake stability, mixing and productivity than are currently possible from individual records alone. This approach to reconstructing seasonal to decadal climate variability will also make paleoclimate reconstructions more valuable as forecasting tools for future climate change impacts on water resources and heat stress, and more amenable to comparison with future climate model simulations.

## 5. Conclusions

In this study we demonstrate the utility of combining multiple isotopic and sclerochronological techniques to investigate seasonal environmental (and especially climate) variability in Quaternary lacustrine sediments. The contrasting hydrology of wet-dry seasons in the Omo River catchment of Lake Turkana is recorded by isotopic variations in incremental growth bands of freshwater bivalves. In this study we have investigated stable isotope and growth increment sclerochronology, coupled with clumped isotope paleotemperature analysis on Holocene *Etheria elliptica* (African river oyster) and Early Pleistocene (1.6 Ma) *Pseudobovaria* sp. bivalves. We have compared modern materials with samples from outcrops and a drill core from various locations around the northern part of Lake Turkana, and also with earlier similar data sets from Vonhof et al. (2013). Deltaic shells exhibit broad isotopic variability (~5–7‰ range within individual shells), with negative  $\delta^{18}\text{O}_s$  values reflecting Omo River discharge coeval with Ethiopian Highland monsoonal precipitation and the most positive  $\delta^{18}\text{O}_s$  values reflecting highly evaporated lake water during the dry seasons and reduced river input. Exclusively riverine or lacustrine shells exhibit narrower seasonal isotopic variability. The large seasonal range in  $\delta^{18}\text{O}_s$  of Late Holocene (i.e. 400 - 500 cal. yr. BP) *E. elliptica* suggests a deltaic environment at the location of shell growth, with highly seasonal Omo River runoff comparable to modern discharge regimes and hydroclimate of the Omo-Turkana Basin. In addition, the highest  $\delta^{18}\text{O}_w$  values calculated for any of our samples occur in the Late Holocene shells, suggesting that open lake water was highly evaporated in this interval, more than that of the modern lake or any other interval sampled by our shells. Middle Holocene (5300–5800 cal. yr. BP) *E. elliptica* exhibit a small seasonal range in  $\delta^{18}\text{O}_s$  at end of the AHP. The limited seasonal isotopic variability of these lacustrine shells is likely a dampened response of river discharge into a fresher lake during an overall wetter climate regime, an idea supported by lower  $\delta^{18}\text{O}_w$  values derived from these shells in comparison to those from the modern lake. Somewhat surprisingly, these specimens with low intra-shell variability were growing at the end of the AHP, a time marked by century-millennial scale climatic instability with rapid lake level fluctuations, but age control uncertainties confound the exact timing of lake level highstands/lowstands. The complex paleohydrology at the termination of the AHP may have resulted from an interaction of orbital insolation changes and millennial-scale climate events. The single Middle Holocene *E. elliptica* shell for which we have growth band data does not demonstrate any statistically significant relationships between growth increments and



stable isotopes. This may imply that *E. elliptica* shell growth is relatively constant in this thermally non-seasonal climate, and growth rates are not strongly affected by seasonal changes in Omo River runoff. Our results suggest surface water temperatures similar to modern may have prevailed during the Middle and Late Holocene, and the combination of clumped isotope paleotemperatures from surface dwelling *E. elliptica* with TEX<sub>86</sub>-based paleotemperature estimates originating at the base of the water column mixed zone provides a new approach to determining past whole-water column temperature range, which in turn may be a useful proxy for thermal seasonality (Fig. 7b).

Early Pleistocene *Pseudobovaria* sp. exhibit a large seasonal range in  $\delta^{18}\text{O}_s$ , suggesting deltaic growth under significant seasonality in paleo-Omo River runoff. High seasonality of Omo River runoff into paleo-lake Lorenyang  $\sim 1.6$  Ma may reflect a situation similar to modern hydroclimate conditions. A deltaic shell  $\sim 1.9$  Ma exhibits a smaller seasonal range in  $\delta^{18}\text{O}_s$  with more negative values than deltaic shells from this study, suggesting increased wet-dry seasonal hydrological variability in the catchment of Paleolake Lorenyang  $\sim 1.6$  Ma as compared to  $\sim 1.9$  Ma. Limited clumped isotope paleotemperature data from these same shells suggest that both cooler and more variable near surface water conditions may have prevailed at 1.6 Ma compared to the present. Environmental changes in hydroclimate seasonality would have impacted vegetation cover, habitat type, resource and freshwater availability, and in turn may have exerted selective pressures on eastern African terrestrial mammals, including hominins, to adapt and migrate in response to seasonal variation in water availability during the Early Pleistocene. Using the approach we lay out here, future combined sclerochronology/isotope/clumped isotope studies in the Turkana Basin and elsewhere, using larger and more temporally continuous data sets, could explore the timing and rates of change in river discharge as an indication of variable flood pulse strength, and indirectly of changing seasonality in precipitation for upland watersheds. When combined with fully lacustrine records (away from directly proximal deltaic influence) such records could also provide a window into how lake systems are responding to regional climate forcing. This would be further strengthened by both clumped isotope records from sublittoral/profundal mollusks and TEX<sub>86</sub> metalimnetic records of deeper water temperatures (Fig. 7b), allowing us to track through time the evolution of lake water column thermal structure and stability, and how these change on sub-annual timescales. Sclerochronological data, in combination with isotopic records of lake-water variability, provide an important tool for inferring past seasonality and thereby addressing questions about the response of past ecosystems to such short-time duration climate variability.

#### Author contributions

All authors have made substantial contributions to this manuscript.

1) Andrew Cohen, Julia Manobianco, Bryan Black and David Dettman designed the research, 2) Andrew Cohen, Craig Feibel, Bert Van Bocxlaer and Josephine Joordens collected and/or provided fossil samples analyzed in the study, 3) Julia Manobianco, Andrew Cohen and David Dettman conducted the research and generated data used in the research, 4) Andrew Cohen and Julia Manobianco wrote the initial versions of the manuscript, 5) All authors edited subsequent versions of the manuscript.

#### Declaration of competing interest

The authors declare that they have no known competing financial interests or personal relationships that could have appeared to influence the work reported in this paper.

#### Data availability

Data will be made available on request.

#### Acknowledgements

Field work for this research was authorized by the Kenyan National Council for Science and Technology. This research was conducted as part of the

Hominin Sites and Paleolakes Drilling Program (HSPDP). Initial WTK13 core processing and

sampling was completed at the Continental Scientific Drilling (CSD) Facility, University of Minnesota, USA, and the WTK13 core is archived at CSD. Funding for this work was provided by National Science Foundation (NSF) grants EAR-1123942, BCS-1241859, EAR-1338553, and the International Continental Scientific Drilling Program (ICDP). BVB acknowledges support from the 80|Prime project EnviroMolSed funded by the French National Center for Scientific Research (CNRS). We thank Stephanie Kukolich for assistance with shell micromilling and fine-scale sampling, and David Edge for assistance with imaging. We also thank two anonymous reviewers for very helpful suggestions on improving this paper. This is HSPDP Publication #54.

#### Appendix A. Supplementary data

Supplementary data to this article can be found online at <https://doi.org/10.1016/j.quascirev.2023.108284>.

#### References

- Abell, P.I., Ameghshitsi, L., Ochumba, P.B.O., 1995. The shells of *Etheria elliptica* as seasonal recorders at Lake Victoria. *Palaeogeog., Palaeoclim. Palaeoecol.* 119, 215–219.
- Abell, P., Hoelzmann, P., 2000. Holocene palaeoclimates in northwestern Sudan: stable isotope studies on molluscs. *Global Planet. Change* 26, 1–12.
- Aké, G.D., Agadjihouédé, H., Mensah, G.A., Lalèyè, P.A., 2015. Population dynamics of freshwater oyster *Etheria elliptica* (Bivalvia: Etheriidae) in the Pendjari River (Benin-western Africa). *Knowl. Mgmt. Aquatic Ecosyst* 416, 6. <https://doi.org/10.1051/kmae/2015002>.
- Anderson, N.T., Kelson, J.R., Kele, S., Daëron, S., Bonifacie, M., Horita, J., Mackey, T.J., John, C.M., Kluge, T., Petschnig, P., Jost, A.B., Huntington, K.W., Bernasconi, S.M., Bergmann, K.D., 2021. A unified clumped isotope thermometer calibration (0.5–1,100°C) using carbonate-based standardization. *Geophys. Res. Lett.* 48. <https://doi.org/10.1029/2020GL092069>.
- Anthony, J.L., Kesler, D.H., Downing, W.L., Downing, J.A., 2001. Length-specific growth rates in freshwater mussels (Bivalvia: Unionidae): extreme longevity or generalized growth cessation? *Freshw. Biol.* 46, 1349–1359.
- Avery, S.T., Tebbis, E.J., 2018. Lake Turkana, major Omo River developments, associated hydrological cycle change and consequent lake physical and ecological change. *J. Great Lake. Res.* 44, 1164–1182.
- Beck, C.C., Feibel, C.S., Henderek, R.L., Cohen, A.S., Campisano, C.J., 2015. Members of the HSPDP Project Team, 2015. A facies interpretation of the Hominin Sites and Paleolakes Drilling Project West Turkana core: Dynamic fluctuations on a shallow lacustrine margin. *Vith International Limnogeology Congress*, Reno, NV.
- Beck, C.C., Feibel, C.S., Wright, J.D., Mortlock, R.A., 2019. Early onset for the African Humid Period at Kabua Gorge, Turkana Basin, Kenya. *The Holocene* 29, 1011–1019.
- Berke, M.A., Johnson, T.C., Werne, J.P., Grice, K., Schouten, S., Sinninghe Damsté, J.S., 2012. Molecular records of climate variability and vegetation response since the late Pleistocene in the Lake Victoria basin, east Africa. *Quat. Sci. Rev.* 55, 59–74.
- Bloszies, C., Forman, S.L., Wright, D.K., 2015. Water level history for Lake Turkana, Kenya in the past 15,000 years and a variable transition from the African Humid Period to Holocene aridity. *Global Planet. Change* 132, 64–76.
- Boës, X., Prat, S., Arrighi, V., Feibel, C., Haileab, B., Lewis, J., Harmand, S., 2018. Lake-level changes and hominin occupations in the arid Turkana basin during volcanic closure of the Omo River outflows to the Indian Ocean. *Quat. Res.* 2, 892–909. <https://doi.org/10.1017/qua.2018.118>.
- Bonnefille, R., Umer, M., 1994. Pollen-inferred climatic fluctuations in Ethiopia during the last 3,000 years. *Palaeogeogr. Palaeoclimatol. Palaeoecol.* 109, 331–343.
- Brown, F.H., Feibel, C.S., 1991. Stratigraphy, depositional environments, and palaeogeography of the Koobi Fora Formation. In: Harris, J.M. (Ed.), *Koobi Fora Research Project*, vol. 3. Clarendon Press, Oxford, pp. 1–30.
- Butzer, K., Thurber, B., 1969. Some late Cenozoic sedimentary formations of the lower Omo basin. *Nature* 222, 1132–1143.
- Cerling, T.E., Bowman, J.R., O'Neil, J.R., 1988. An isotopic study of a fluvial-lacustrine sequence: The Plio-Pleistocene Koobi Fora sequence, East Africa. *Palaeogeogr. Palaeoclimatol. Palaeoecol.* 4, 335–356. [https://doi.org/10.1016/0031-0182\(88\)90104-9](https://doi.org/10.1016/0031-0182(88)90104-9).
- Cohen, A.S., 1986. Distribution and Faunal Associations of Benthic Invertebrates at Lake Turkana, Kenya. *Hydrobiologia* 74, 179–197.
- Cohen, A.S., 1989. The taphonomy of gastropod shell accumulations in large lakes: an example from Lake Tanganyika, Africa. *Paleobiology* 15, 26–45.

- Cohen, A., Campisano, C., Arrowsmith, R., Asrat, A., Behrensmeier, A.K., Deino, A., Feibel, C., Hill, A., Johnson, R., Kingston, J., Lamb, H., Lowenstein, T., Noren, A., Olago, D., Owen, R.B., Potts, R., Reed, K., Renaut, R., Schabitz, F., Tiercelin, J.-J., Trauth, M.H., Wynn, J., Ivory, S., Brady, K., O'Grady, R., Rodysill, J., Githiri, J., Russell, J., Foerster, V., Dommain, R., Rucina, S., Deocampo, D., Russell, J., Billingsley, A., Beck, C., Dorenbeck, G., Dullo, L., Feary, D., Garello, D., Gromig, R., Johnson, T., Junginger, A., Karanja, M., Kimburi, E., Mbuthia, A., McCartney, T., McNulty, E., Muiruri, V., Nambiro, E., Negash, E.W., Njagi, D., Wilson, J.N., Rabideaux, N., Raub, T., Sier, M.J., Smith, P., Urban, J., Warren, M., Yadeta, M., Yost, C., Zinaye, B., 2016a. The Hominin Sites And Paleolakes Drilling Project: inferring the environmental context of human evolution from eastern African Rift lake deposits. *Sci. Drill.* 21, 1–16. <https://doi.org/10.5194/sd-21-1-2016>.
- Cohen, A.S., Gergurich, E.L., Kraemer, B.M., McGlue, M.M., McIntyre, P.B., Russell, J.M., Simmons, J.D., Swarzenski, R.W., 2016b. Climate warming reduces fish production and benthic habitat in Lake Tanganyika, one of the most biodiverse freshwater ecosystems. *Proc. Natl. Acad. Sci. USA* 113, 9563–9568.
- Cohen, A.S., Du, A., Rowan, J., Yost, C.L., Billingsley, A.L., Campisano, C.J., Brown, E.T., Deino, A.L., Feibel, C.S., Grant, K., Kingston, J.D., Lupien, R., Muiruri, V., Owen, R. B., Reed, K.E., Russell, J., Stockhecke, M., 2022. Plio-Pleistocene African environmental variability and mammalian evolution. *Proc. Natl. Acad. Science* 119 (16), e2107393119.
- Daeron, M., 2021. Full propagation of analytical uncertainties in  $\Delta_{47}$  measurements. *Geochemistry, geophysics. Geosystems* 22. <https://doi.org/10.1029/2020GC009592>.
- de Menocal, P., Ortiz, J., Guilderson, T., Adkins, J., Sarnthein, M., Baker, L., Yarusinsky, M., 2000. Abrupt onset and termination of the African Humid Period: rapid climate responses to gradual insolation forcing. *Quat. Sci. Rev.* 19 (1–5), 347–361. [https://doi.org/10.1016/S0277-3791\(99\)00081-5](https://doi.org/10.1016/S0277-3791(99)00081-5).
- Dettman, D.L., Reische, A.K., Lohmann, K.C., 1999. Controls on the stable isotope composition of seasonal growth bands in aragonitic fresh-water bivalves (Unionidae). *Geochem. Cosmochim. Acta* 7–8, 1049–1057. [https://doi.org/10.1016/S0016-7037\(99\)00020-00024](https://doi.org/10.1016/S0016-7037(99)00020-00024).
- Dettman, D.L., Kohn, M.J., Quade, J., Ryerson, F.J., Ojha, T.P., Hamidullah, S., 2001. Seasonal stable isotope evidence for a strong Asian monsoon throughout the past 10.7 m.y. *Geology* 29, 31–34. [https://doi.org/10.1130/0091-7613\(2001\)029<0031SSIEFA>2.0.CO;2](https://doi.org/10.1130/0091-7613(2001)029<0031SSIEFA>2.0.CO;2).
- de Winter, N.J., Goderis, S., Van Malderen, S.J.M., Sinnesal, M., Vansteenberge, S., Snoeck, C., Belza, J., Vanhaecke, F., Claeys, P., 2020. Subdaily-scale chemical variability in a *Torreites sanchezii* rudist shell: implications for rudist paleobiology and the Cretaceous day-night cycle. *Paleoceanogr. Palaeoclimatol.* 35 <https://doi.org/10.1029/2019PA003723>.
- Downing, W.L., Downing, J.A., 1993. Molluscan shell growth and loss. *Nature* 362, 506.
- Elderkin, C.L., Clewing, C., Ndeo, O.W., Albrecht, C., 2016. Molecular phylogeny and DNA barcoding confirm cryptic species in the African freshwater oyster *Etheria elliptica* Lamarck, 1807 (Bivalvia: Etheriidae). *Biol. J. Linn. Soc.* 118 (2), 369–381. <https://doi.org/10.1111/bj.12734>.
- Epstein, S., Buchsbaum, R., Lowenstam, H.A., Urey, H.C., 1953. Revised carbonate–water isotopic temperature scale. *Bull. Geol. Soc. Am.* 64, 1315–1326.
- Escobar, J., Curtis, J.H., Brenner, M., Hodell, D.A., Holmes, J.A., 2010. Isotope measurements of single ostracod valves and gastropod shells for climate reconstruction: evaluation of within-sample variability and determination of optimum sample size. *J. Paleolimnol.* 43, 921. <https://doi.org/10.1007/s10933-009-9377-9>.
- Ethiopia Electric Power Corporation EEPCCO, 2009. Environmental and social impact assessment: Gibe III project. CESI SpA - Mid-Day Int. Consult. Eng.
- Faith, J.T., Du, A., Behrensmeier, A.K., Davies, B., Patterson, D.B., Rowan, J., Wood, B., 2021. Rethinking the ecological drivers of hominin evolution. *Trends Ecol. Evol.* 36, 797–807.
- Fan, M., Dettman, D.L., 2009. Late Paleocene high Laramide ranges in northeast Wyoming: Oxygen isotope study of ancient river water. *Earth Planet Sci. Lett.* 286, 110–121. <https://doi.org/10.1016/j.epsl.2009.06.024>.
- Feibel, C.S., 1994. Freshwater stingrays from the Plio-Pleistocene of the Turkana Basin, Kenya and Ethiopia. *Lethaia* 26, 359–366.
- Feibel, C.S., 2011. A geological history of the Turkana Basin. *Evolutionary anthropology. Issues, News, and Rev.* 20, 206–216.
- Ferguson, A.J.D., Harbott, B.J., 1972. Geographical, physical, and chemical aspects of Lake Turkana. In: Hopson, A.J. (Ed.), *Lake Turkana: a Report on the Findings of the Lake Turkana Project, 1972–1975*. Overseas Development Administration, London, pp. 1–108.
- Ficken, K.J., Woodler, M.J., Swain, D.L., Street-Perrott, F.A., Eglinton, G., 2002. Reconstruction of a subalpine grass-dominated ecosystem, Lake Rutundu, Mount Kenya: a novel multi-proxy approach. *Paleoceanogr. Palaeoclimatol. Palaeoecol.* 177, 137–149.
- Fischer, M.L., Markowska, M., Bachofer, F., Foerster, V.E., Asrat, A., Zielhofer, C., Trauth, M.H., Junginger, A., 2020. Determining the pace and magnitude of Lake level changes in southern Ethiopia over the last 20,000 Years using lake balance modeling and SEBAL. *Front. Earth Sci.* <https://doi.org/10.3389/feart.2020.00197>.
- Foerster, V., Vogelsang, R., Junginger, A., Asrat, A., Lamb, H.F., Schabitz, F., Trauth, M. H., 2015. Environmental change and human occupation of southern Ethiopia and northern Kenya during the last 20,000 years. *Quat. Sci. Rev.* 129, 333–340. <https://doi.org/10.1016/j.quascirev.2015.10.026>.
- Forman, S.L., Wright, D.K., Blaszies, C., 2014. Variations in water level for Lake Turkana in the past 8500 years near Mt. Porr, Kenya and the transition from the African Humid Period to Holocene aridity. *Quat. Sci. Rev.* 97, 84–101. <https://doi.org/10.1016/j.quascirev.2014.05.005>.
- Garcin, Y., Melnick, D., Strecker, M.R., Olago, D., Tiercelin, J.J., 2012. East African mid-Holocene wet–dry transition recorded in palaeo-shorelines of Lake Turkana, northern Kenya Rift. *Earth Planet Sci. Lett.* 331–332, 322–334.
- Glaubke, R.H., Thirumalai, K., Schmidt, M.W., Hertzberg, J.E., 2021. Discerning changes in high-frequency climate variability using geochemical populations of individual foraminifera. *Paleoceanogr. Palaeoclimatol.* 36, e2020PA004065 <https://doi.org/10.1029/2020PA004065>.
- Gröcke, D.R., Gillikin, D.P., 2008. Advances in mollusc sclerochronology and sclerochemistry: tools for understanding climate and environment. *Geo Mar. Lett.* 28, 265–268. <https://doi.org/10.1007/s00367-008-0108-4>.
- Grossman, E.L., Ku, T.-L., 1986, 59. In: *Oxygen and Carbon Isotope Fractionation in Biogenic Aragonite: Temperature Effects*. *Chem. Geol.: Isotope Geoscience Section*, pp. 59–74. [https://doi.org/10.1016/0168-9622\(86\)90057-6](https://doi.org/10.1016/0168-9622(86)90057-6).
- Grove, M., 2011. Change and variability in Plio-Pleistocene climates: modelling the hominin response. *J. Archaeol. Sci.* 38, 3038–3047. <https://doi.org/10.1016/j.jas.2011.07.002>.
- Halfman, J.D., Johnson, T.C., Finney, B.P., 1994. New AMS dates, stratigraphic correlations and decadal climatic cycles for the past 4-ka at Lake Turkana, Kenya. *Paleoceanogr. Palaeoclimatol. Palaeoecol.* 111, 83–98.
- Hallman, N., Burchell, M., Brewster, N., Martindale, A., Schone, B.R., 2013. Holocene climate and seasonality of shell collection at the Dundas Islands Group, northern British Columbia, Canada—A bivalve sclerochronological approach. *Paleogeography Palaeoclimatology Palaeoecology* 373, 163–172.
- Hammer, Ø., 2020. PAST Paleontological Statistics. <https://past.en.fo4d.com/windows>.
- Huang, Y., Street-Perrott, F.A., Perrott, R.A., Metzger, P., Eglinton, G., 1999. Glacial-Interglacial environmental changes inferred from molecular and compound-specific  $\delta^{13}C$  analyses of sediments from Sacred Lake. Mt. Kenya. *Geochim. Cosmochim. Acta* 63, 1383–1404.
- Johnson, T.C., Malala, J.O., 2009. Lake Turkana and Its link to the Nile. In: Dumont, H. (Ed.), *The Nile*, pp. 287–304. [https://doi.org/10.1007/978-1-4020-9726-3\\_15](https://doi.org/10.1007/978-1-4020-9726-3_15). Springer Netherlands.
- Joordens, J.C.A., Vonhof, H.B., Feibel, C.S., Lourens, L.J., Dupont-Nivet, G., van der Lubbe, J.H.J.L., Sier, M.J., Davies, G.R., Kroon, D., 2011. An astronomically-tuned climate framework for hominins in the Turkana Basin. *Earth Planet Sci. Lett.* 1–2, 1–8.
- Joordens, J., Feibel, C., Vonhof, H., Schulp, A., Kroon, D., 2019. Relevance of the eastern African coastal forest for early hominin biogeography. *J. Hum. Evol.* 131, 176–202.
- Junginger, A., Trauth, M.H., 2013. Hydrological constraints of paleo-lake Suguta in the northern Kenya rift during the African Humid Period (15–5 ka BP). *Global Planet. Change* 111, 174–188.
- Junginger, A., Roller, S., Olaka, L.A., Trauth, M.H., 2014. The effects of solar irradiation changes on the migration of the Congo Air Boundary and water levels of paleo-lake Suguta, northern Kenya rift, during the African Humid Period (15–5ka BP). *Paleoceanogr., Palaeoclim. Palaeoecol.* 396, 1–16. <https://doi.org/10.1016/j.paleo.2013.12.007>.
- Kaboth-Bahr, S., Gosling Vogelsang, R.W., Bahr, A., Scerri, E.M.L., Asrat, A., Cohen, A.S., Düsing, W., Foerster, V., Lamb, H.F., Maslin, M.A., Roberts, H.M., Schabitz, F., Trauth, M.H., 2021. Paleo-ENSO influence on African environments and early modern humans. *Proc. Natl. Acad. Sci. USA* 118, 23. <https://doi.org/10.1073/pnas.2018277118>.
- Källqvist, T., Lien, L., Liti, D., 1988. Lake Turkana limnological study 1985–1988. Norwegian Inst. For Water Res. (NIVA) 98. Report D-B5313.
- Kelemen, Z., Gillikin, D.P., Bouillon, S., 2019. Relationship between river water chemistry and shell chemistry of two tropical African freshwater bivalve species. *Chem. Geol.* 526, 130–141. <https://doi.org/10.1016/j.chemgeo.2018.04.026>.
- Kim, J.-H., van der Meer, J., Schouten, S., Helmke, P., Willmott, V., Sangiorgi, F., Koç, N., Hopmans, E.C., Damsté, J.S.S., 2010. New indices and calibrations derived from the distribution of crenarchaeal isoprenoid tetraether lipids: implications for past sea surface temperature reconstructions. *Geochem. Cosmochim. Acta* 74, 4639–4654.
- Kingston, J.D., Deino, A., Hill, A., Edgar, R., 2007. Astronomically forced climate change in the Kenyan Rift Valley 2.7–2.55 Ma: implications for the evolution of early hominin ecosystems. *J. Hum. Evol.* 53, 487–503.
- Kraemer, B.M., Hook, S., Huttula, T., Kotilainen, P., O'Reilly, C.M., Peltonen, A., Plisnier, P.D., Sarvala, J., Tamatamah, R., Vadeboncoeur, Y., Wehrli, B., McIntyre, P. B., 2015. Century-long warming trends in the upper water column of Lake Tanganyika. *PLoS One* 10 (7), e0132490. <https://doi.org/10.1371/journal.pone.0132490>.
- Levin, N.E., 2015. Environment and climate of early human evolution. *Annu. Rev. Earth Planet Sci.* 43, 405–429.
- Levin, N.E., Zipser, E.J., Cerling, T.E., 2009. Isotopic composition of waters from Ethiopia and Kenya: insights into moisture sources for eastern Africa. *D23 J. Geophys. Res.* <https://doi.org/10.1029/2009jd012166>.
- Lupien, R.L., Russell, J.M., Feibel, C., Beck, C., Castañeda, I., Deino, A., Cohen, A.S., 2018. A leaf wax biomarker record of early Pleistocene hydroclimate from West Turkana, Kenya. *Quat. Sci. Rev.* 186, 225–235. <https://doi.org/10.1016/j.quascirev.2018.03.012>.
- Lupien, R.L., Russell, J.M., Grove, M., Beck, C.C., Feibel, C.S., Cohen, A.S., 2020. Impacts of abrupt and high-frequency climate change on hominin evolution during the early Pleistocene in the Turkana Basin, Kenya. *Quat. Sci. Rev.* 245 <https://doi.org/10.1016/j.quascirev.2020.106531>.
- Mandahl-Barth, G., 1988. Studies on African freshwater bivalves. In: Kristensen, K., Svenningsen, E. (Eds.), *Danish Bilharziasis Laboratory, Charlottenlund, Denmark*, pp. 1–161.
- Maxwell, S.J., Hopley, P.J., Upchurch, P., Soligo, C., 2018. Sporadic sampling, not climatic forcing, drives observed early hominin diversity. *Proc. Natl. Acad. Sci. USA* 115, 4891–4896.

- McGlue, M.M., Soreghan, M.J., Michel, E., Todd, J.A., Cohen, A.S., Mischler, J., O'Connell, C.S., Castaneda, O.S., Hartwell, R.J., Nkotagu, H.N., Lezzar, K.E., 2009. Environmental controls on rift lake shell carbonates: a view from Lake Tanganyika's littoral. *Palaios* 2, 426–438.
- Morrissey, A., Scholz, C.A., 2014. Paleohydrology of Lake Turkana and its influence on the Nile River system. *Palaeogeog., palaeoclim. Palaeoecol.* 403, 88–100. <https://doi.org/10.1016/j.palaeo.2014.03.029>.
- Morrissey, A., Scholz, C.A., Russell, J.M., 2018. Late Quaternary TEX<sub>86</sub> paleotemperatures from the world's largest desert lake, Lake Turkana, Kenya. *J. Paleolimnol.* 59, 103–117. <https://doi.org/10.1007/s10933-016-9939-6>.
- Ng'ang'a, P., Muchane, M.W., Johnson, T.C., Sturgeon, K., 1998. Comparison of isotopic records in abiogenic and biogenic calcite from Lake Turkana, Kenya. In: Lehman, J. T. (Ed.), *Environmental Change and Response in East African Lakes*. Monographiae Biologicae, vol. 79. Springer, Dordrecht, pp. 173–190. [https://doi.org/10.1007/978-94-017-1437-2\\_14](https://doi.org/10.1007/978-94-017-1437-2_14).
- Nicholson, S.E., 1996. A review of climate dynamics and climate variability in eastern Africa. In: Johnson, T., Odada, E. (Eds.), *The Limnology, Climatology and Paleoclimatology of the East African Lakes*. Gordon and Breach, Amsterdam, pp. 25–56.
- Nicholson, S.E., 2018. The ITCZ and the seasonal cycle over equatorial Africa. *Bull. Amer. Met. Soc.* 99 (2), 337–348. [10.1175/BAMS-D-16-0287.1](https://doi.org/10.1175/BAMS-D-16-0287.1).
- Nutz, A., Schuster, M., Boës, X., Rubino, J.L., 2017. Orbitally-driven evolution of Lake Turkana (Turkana depression, Kenya, East African Rift System): paleolake fluctuations, paleolandscapes and controlling factors. *Earth Sci. Rev.* 211, 103415. <https://doi.org/10.1016/j.jafrearsci.2016.10.016>.
- Nutz, A., Schuster, M., Barboni, D., Gassier, G., Van Bocxlaer, B., Robin, C., Ragon, T., Ghienne, J.F., Rubino, J.L., 2020. Plio-Pleistocene sedimentation in West Turkana (Turkana depression, Kenya, East African Rift System): paleolake fluctuations, paleolandscapes and controlling factors. *Earth Sci. Rev.* 211, 103415. <https://doi.org/10.1016/j.jafrearsci.2020.103415>.
- Ortiz-Sepulveda, C., Stelbrink, B., Vekemans, X., Albrecht, C., Riedel, F., Todd, J., Van Bocxlaer, B., 2020. Diversification dynamics of freshwater bivalves (Unionidae: Parreysiinae: Coelaturini) indicate historic hydrographic connections throughout the East African Rift System. *Mol. Phylogenet. Evol.* 148 <https://doi.org/10.1016/j.ympev.2020.106816>.
- Passay, B., Levin, N., Cerling, T., Eiler, J., 2010. High-temperature environments of human evolution in East Africa based on bond ordering in paleosol carbonates. *Proc. Natl. Acad. Sci. USA* 107, 11245–11249.
- Plisnier, P.D., Serneels, S., Lambin, E.F., 2000. Impact of ENSO on East African ecosystems: a multivariate analysis based on climate and remote sensing data. *Global Ecology and Biogeography* 9, 481–497.
- Potts, R., 1996. Evolution and climate variability. *Science* 273, 922–923.
- Potts, R., Faith, J.T., 2015. Alternating high and low climate variability: the context of natural selection and speciation in Plio-Pleistocene hominin evolution. *J. Hum. Evol.* 87, 5–20.
- Reimer, P., Austin, W., Bard, E., Bayliss, A., Blackwell, P., Bronk Ramsey, C., Talamo, S., 2020. The IntCal20 northern hemisphere radiocarbon age calibration curve (0–55 cal kBP). *Radiocarbon* 62, 725–757. <https://doi.org/10.1017/RDC.2020.41>.
- Ricketts, R.D., Johnson, T.C., 1996. Climate change in the Turkana basin as deduced from a 4000 year long δO<sub>18</sub> record. *Earth Planet Sci. Lett.* 1–2, 7–17. [https://doi.org/10.1016/0012-821x\(96\)00094-5](https://doi.org/10.1016/0012-821x(96)00094-5).
- Rodrigues, D., Abell, P.L., Kröpelin, S., 2000. Seasonality in the early Holocene climate of Northwest Sudan: interpretation of *Etheria elliptica* shell isotopic data. *Global Planet. Change* 26, 181–187. [https://doi.org/10.1016/S0921-8181\(00\)00043-6](https://doi.org/10.1016/S0921-8181(00)00043-6).
- Schouten, S., Hopmans, E.C., Schefuss, E., Sinninghe Damste, J.S., 2002. Distributional variations in marine crenarchaeal membrane lipids: a new tool for reconstructing ancient sea water temperatures? *Earth Planet Sci. Lett.* 204, 265–274.
- Sharp, Z., 2007. *Principles of Stable Isotope Geochemistry* Pearson, p. 344.
- Sier, M.J., Langereis, C.G., Dupont-Nivet, G., Feibel, C.S., Joordens, J.C.A., van der Lubbe, J.H.J.L., Beck, C.C., Olago, D., Cohen, A.S., WTK Science Team Members, 2017. The top of the olduvai subchron in a high resolution magnetostratigraphy from the West Turkana core WTK13, Hominin Sites and Paleolakes Drilling Project (HSPDP). *Quat. Geochronol.* 42, 117–129.
- Soreghan, M.R., Cohen, A.S., Bright, J.E., Kaufman, D.S., McGlue, M., Kimirei, I., 2021. Time Averaging of Shell Beds in Lake Tanganyika, Africa; Implications for a Biodiverse and Threatened Ecosystem. AGU National Meeting, New Orleans. GC45N-0965.
- Street, F.A., Grove, A.S., 1979. Global maps of lake-level fluctuations since 30000 BP. *Quat. Res.* 12, 83–118.
- Thirumalai, K., Cohen, A.S., Taylor, D., 2023. Climatic controls on individual ostracode stable isotopes in a desert lake: a modern baseline for Lake Turkana. G-cubed 24, e2022GC010790. <https://doi.org/10.1029/2022GC010790>.
- Tiercelin, J.J., Lezzar, K.E., 2002. A 300 million year history of rift lakes in Central and East Africa: an updated broad review. In: Odada, E., Olago, D. (Eds.), *The East African Great Lakes: Limnology, Paleolimnology and Biodiversity*. Kluwer Acad. Publ, Dordrecht, The Netherlands, pp. 3–60.
- Tierney, J.E., Russell, J.M., Sinninghe Damsté, J.S., Huang, Y., Verschuren, D., 2011. Late Quaternary behavior of the East African monsoon and the importance of the Congo Air Boundary. *Quat. Sci. Rev.* 30, 798–807.
- Van Bocxlaer, B., 2020. Paleoeological insights from fossil freshwater mollusks of the Kanapoi Formation (Omo-Turkana basin, Kenya). *J. Hum. Evol.* 140 <https://doi.org/10.1016/j.jhevol.2017.05.008>.
- Van Bocxlaer, B., Van Damme, D., 2009. Palaeobiology and evolution of the late Cenozoic freshwater mollusks of the Turkana Basin: Iridinidae Swainson, 1849 and Etheriidae Deshayes, 1830 (Bivalvia: Etherioidea). *J. Syst. Palaeontol.* 2, 129–161. <https://doi.org/10.1017/S1477201908002587>.
- Van Bocxlaer, B., Salenbien, W., Praet, N., Verniers, J., 2012. Stratigraphy and paleoenvironments of the early to middle Holocene Chipalawamba Beds (Malawi basin, Africa). *Biogeosciences* 9, 4497–4512.
- van der Lubbe, J.H.J.L., Krause-Nehring, J., Junginger, A., Garcin, Y., Joordens, J.C.A., Davies, G.R., Beck, C., Feibel, C.S., Johnson, T.C., Vonnhof, H.B., 2017. Gradual or abrupt? Changes in water source of Lake Turkana during the African Humid Period inferred from Sr isotope ratios. *Quat. Sci. Rev.* 174, 1–12.
- Velarde, A.A., Flye-Sainte-Marie, J., Mendo, J., Jean, F., 2015. Sclerochronological records and daily microgrowth of the Peruvian scallop (*Argopecten purpuratus*, Lamarck, 1819) related to environmental conditions in Paracas Bay, Pisco, Peru. *J. Sea Res.* 99, 1–8. <https://doi.org/10.1016/j.seares.2015.01.002>.
- Vonnhof, H.B., Joordens, J.C.A., Noback, M.L., van der Lubbe, J.H.J.L., Feibel, C.S., Kroon, D., 2013. Environmental and climatic control on seasonal stable isotope variation of freshwater molluscan bivalves in the Turkana Basin (Kenya). *Palaeogeog., Palaeoclim. Palaeoecol.* 383–384, 16–26. <https://doi.org/10.1016/j.palaeo.2013.04.022>.
- Wang, X., Dettman, D.L., Wang, M., Zhang, J., Saito, Y., Quade, J., Feng, S., Liu, J., Chen, F., 2020. Seasonal wet-dry variability of the Asian monsoon since the Middle Pleistocene. *Quat. Sci. Rev.* 247 <https://doi.org/10.1016/j.quascirev.2020.106568>.
- Wood, B., Leakey, M., 2011. The Omo-Turkana Basin fossil hominins and their contribution to our understanding of human evolution in Africa. *Evol. Anthropol.* 20, 264–292.
- Yanay, N., Wang, Z., Dettman, D.L., Quade, J., Huntington, K.W., Schauer, A.J., Nelson, D.D., McManus, J.B., Thirumalai, K., Sakai, S., Morillo, A.R., Mallik, A., 2022. Rapid and precise measurement of carbonate clumped isotopes using laser spectroscopy. *Sci. Adv.* 8. <https://doi.org/10.1126/sciadv.abq0611>.
- Yang, H., Gu, X., Gibbs, R.B., Evans, S.H., Downs, R.T., Jibrin, Z., 2022. Lazaraskeite, Cu (C<sub>2</sub>H<sub>3</sub>O<sub>3</sub>)<sub>2</sub>, the First Organic Mineral Containing Glycolate, from the Santa Catalina Mountains, vol. 107. *American Mineralogist*, Tucson, Arizona, U.S.A, pp. 509–516. <https://doi.org/10.2138/am-2021-7895>.
- Yang, W., Seager, R., Cane, M.A., Lyon, B., 2015. The annual cycle of East African precipitation. *J. Clim.* 28, 2385–2404. <https://doi.org/10.1175/JCLI-D-14-00484.1>.
- Yost, C.L., Lupien, R.L., Beck, C., Feibel, C.S., Archer, S.R., Cohen, A.S., 2021. Orbital influence on precipitation, fire, and grass community composition from 1.87 to 1.38 Ma in the Turkana Basin, Kenya. *Frontiers Earth Sci* 9. <https://doi.org/10.3389/feart.2021.568646>.
- Yuretich, R.F., Cerling, T.E., 1983. Hydrogeochemistry of Lake Turkana: mass balance and mineral reactions in an alkaline lake. *Geochem. Cosmochim. Acta* 47, 1099–1109.